



Available online at [www.sciencedirect.com](http://www.sciencedirect.com)

**jmr&t**  
Journal of Materials Research and Technology  
[www.jmrt.com.br](http://www.jmrt.com.br)



## Review Article

# Additive manufacturing of zirconia ceramics: a state-of-the-art review



Xiuping Zhang<sup>a</sup>, Xin Wu<sup>b</sup>, Jing Shi<sup>b,\*</sup>

<sup>a</sup> School of Mechanical and Materials Engineering, Xi'an University, Xi'an, Shaanxi, China

<sup>b</sup> Department of Mechanical & Materials Engineering, College of Engineering and Applied Science, University of Cincinnati, Cincinnati, OH 45221, USA

### ARTICLE INFO

#### Article history:

Received 31 October 2019

Accepted 30 May 2020

Available online 23 June 2020

#### Keywords:

Additive manufacturing

3D Printing

Zirconia ceramic

Performance

Application

### ABSTRACT

In recent years, additive manufacturing (AM) has emerged as a type of efficient manufacturing technology for building ceramic prototypes with increased dimensional accuracy, improved time efficiency, and reduced cost. A wealth of research works have been conducted to uncover the underlying formation mechanism of zirconia ceramic parts manufactured by AM processes and to improve the performance of the parts. In spite of the achievements, there are still some unresolved issues, such as porosity, cracks, coffee staining, which impede the adoption of AM processes for zirconia part manufacturing. This paper aims to review the recent research efforts on zirconia ceramic manufactured using AM techniques. The existing works are mainly categorized in terms of the different AM preparation methods and the applications. More importantly, the challenges and opportunities related to AM of zirconia products are discussed. As such, this review provides not only a comprehensive survey of the existing research, but also an insightful discussion regarding the potential research in the future. Innovations are expected to be stimulated for many critical industrial applications.

© 2020 Published by Elsevier B.V. This is an open access article under the CC BY-NC-ND license (<http://creativecommons.org/licenses/by-nc-nd/4.0/>).

## 1. Introduction

Zirconia is an oxide ceramic material with special crystal structure transition characteristics, i.e., it adopts a monoclinic crystal structure at room temperature and transitions to tetragonal and cubic at higher temperatures [1], which possesses excellent properties such as the high flexural strength,

high fracture toughness, excellent ionic conductivity, thermal and chemical stability, good biocompatibility and corrosion resistance [2–4]. Based on these properties, zirconia ceramics, especially yttrium stabilized zirconia (YSZ), have been paid special attention for industrial and medical applications [5]. For instance, the outstanding mechanical properties (e.g., the compression strength of about 2000 MPa, the bending strength of 900–1200 MPa [3], and the fracture toughness of 5–10 MPa m<sup>1/2</sup> [5]) make zirconia ceramics suitable for the numerous applications of cutting tools, resistive heating elements and oxygen sensors, thread guide, cams, seals, valves, and pump impellers with excellent performance. Thanks to

\* Corresponding author.

E-mail: [jing.shi@uc.edu](mailto:jing.shi@uc.edu) (J. Shi).

<https://doi.org/10.1016/j.jmrt.2020.05.131>

2238-7854/© 2020 Published by Elsevier B.V. This is an open access article under the CC BY-NC-ND license (<http://creativecommons.org/licenses/by-nc-nd/4.0/>).

its extra esthetic characteristics and biocompatibility, zirconia has been very popular in biomedical applications such as surgical implants [6]. Zirconia has also been widely used in dentistry – crowns, bridges, implants, and veneers of zirconia have been successfully adopted at clinics [7,8]. Other applications for zirconia, such as solid oxide fuel cells [9], thermal barrier [10], optical coatings [11], catalysis or catalytic supports [12], and sensors [13], have also been demonstrated in literature.

To fabricate zirconia ceramics for the above applications, various ceramic processing and forming technologies have been adopted, including slip casting, tape-casting, dry pressing, laser cutting, diamond plastic processing, direct consolidation, extrusion, dip coating, microwave irradiation, and injection molding [14–21]. Although zirconia parts can be fabricated, limitations of these conventional techniques still exist. The typical limitations are long production lead time, high labor and cost intensities, high wear rates for the machining tools, low machining accuracy and inability for manufacturing complex shapes [22]. To date, these drawbacks have significantly impeded the industrial utilization of high-strength zirconia ceramic materials in a growing range of engineering and medical disciplines. To overcome the limitations of the conventional manufacturing methods, various attempts have been launched. Additive manufacturing (AM) techniques, also called 3D printing techniques, have emerged as a unique manufacturing philosophy enabling the manufacture of ceramic parts with complex shapes, high precision, and reduced cost [23–25]. As such, the drawbacks existed in conventional zirconia ceramics manufacturing methods can be effectively mitigated. AM processes can be categorized into two different types according to the ISO/ASTM 17296 standard: (i) the single step processes (also called ‘direct’ processes), in which parts are rapidly fabricated in a single operation where the basic geometrical shape and material properties are achieved simultaneously for the intended product, and (ii) the multi-step processes (also called ‘indirect’ processes), in which the parts are fabricated in multiple operations. In general, the same basic principle wherein the final component is fabricated with layer by layer addition of the material could apply to almost all AM techniques [26]. A variety of AM techniques have been adopted to manufacture zirconia ceramics, which include selective laser sintering (SLS), selective laser melting (SLM), stereo-lithography (SLA), ink-jet printing (JP), fused deposition modeling (FDM), and others [27,28]. Despite the significant advances achieved for the manufacturing of zirconia ceramics by AM, the level of maturity of each AM process is different and there are still many issues needed to be resolved. For instance, AM technology is generally not able to reproduce the strength of conventionally produced zirconia ceramics, but the gaps are being closed with the recent advances as indicated by this review paper.

This paper will review the state-of-the-art research progress in applying AM for the fabrication of zirconia ceramics, aiming at stimulating further break-through research in this area. In literature, a few review papers have been published to address the applications of AM technologies for general ceramics [27,29–31], but this is an area of rapid development that requires regular update. More importantly, the existing reviews do not cover enough regarding zirconia mate-

rials, while the research on AM of zirconia ceramics has reached a critical mass which warrants a stand-alone review. To the best of our knowledge, this is the first exclusive review on zirconia by AM. Followed by the introduction, the applications of AM zirconia are summarized in the major industrial fields. Thereafter, the manufacturing of zirconia ceramics by AM is discussed in detail based on the classification of AM methods. Finally, the existing challenges are presented, and future opportunities are pointed out.

## 2. Applications of AM zirconia

Zirconia ceramics have excellent properties such as high toughness [32], thermal insulation [33], biocompatibility [3] and ion conductivity [34], which make them a type of good candidate material for numerous applications. AM technology offers significant advantages for rapid manufacturing needs for complex structures and high-performance products of zirconia ceramic, which could be widely used in aerospace, automotive, marine, energy, biomedical and other fields.

### 2.1. Aerospace and automotive applications

The AM prepared zirconia ceramic parts could deliver unique properties for critical components such as damage isolation, resistance to high temperatures, high strength to density ratios, which are indispensable for many aerospace and automotive applications. Additive manufacturing has the advantage of ultra-high flexibility allowing for the preparation of virtually any shape. For instance, engineers can design the core of turbine blades based on performance optimization without worrying about constraints from traditional manufacturing processes. This brings a new revolution to the blade ceramic core manufacturing process for aerospace/automotive engines.

As early as 2007, Bertrand et al. [35] demonstrated the capability of SLS/SLM for the manufacturing of a turbine blade with accurate geometry based on yttria-zirconia powder. However, the low density of 56% was not sufficient for the application of dental bridges. The impacting factors were also discussed for improving the properties of  $\text{ZrO}_2\text{-Y}_2\text{O}_3$  components. In 2013, Wilkes et al. [36] also employed the SLM process to create zirconia-alumina ceramic parts (41.5 wt.% zirconia, 58.5 wt.% alumina), in which the part was formed free of sintering process. Nearly 100% density was achieved, and the crack formation was avoided by preheating the material to a temperature of at least approximately 1600 °C. Fig. 1 demonstrates a complex shaped ceramic turbine made by SLM, which can be potentially adopted in many aerospace, power generation, and automotive applications. The preheating is able to relieve the formation of cracks and improve material strength for the ceramic turbine, while it could also decrease the surface quality. Then in 2017, Li et al. [37] used laser-melted deposition (LMD) method to fabricate ultrafine nanocrystals (UNs) modified high-entropy alloy composites (HEACs) from the yttria partially stabilized  $\text{ZrO}_2$  (YPSZ) and the FeCoCrAlCu mixed powders, and coated the aviation turbine blade with these composites for enhancing the blade performance. It was demonstrated these composites exhibited finer microstruc-

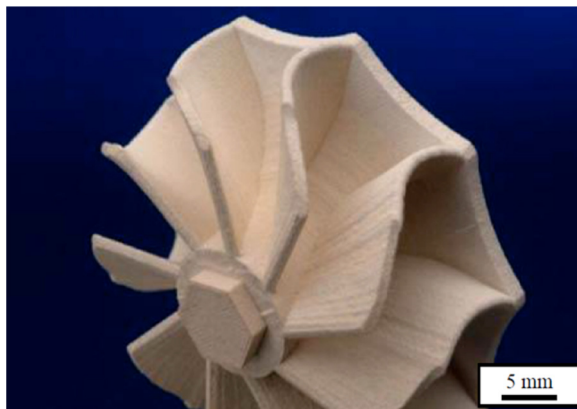


**Fig. 1 – Turbine of a turbocharger made by SLM out of 80 wt.% zirconia/20 wt.% alumina (no preheating) [36].**

ture free of micro-crack under the production of relative stable atomic group of UNs with short-range order. It was further pointed out that due to the existence of such various phases, the laser-induction HEACs exhibited better wear performance than that of the FeCoCrAlCu LMD high-entropy alloy.

## 2.2. Biomedical applications

AM has a strong share of market in medical and dental industry. Currently, numerous medical applications have been realized with the available AM techniques, including scaffolds, human osteosarcoma, blood vessels, cartilage, hip joints, knee joints, bones, and soft tissues [38–43]. Various polymers, alloys, glass and ceramic materials have found their applications as implant materials [44–46]. For instance, Wu et al. [46] adopted the stereolithographic process to obtain dense zirconia-toughened alumina ceramics with excellent properties, comparable to those obtained through conventional techniques. The additional advantage of high customizability of the geometry warrants great application potential in medical implants. Yttria-stabilized tetragonal zirconia polycrystals (Y-TZPs) hold several advantages in fabricating the medical implants. For instance, Y-TZP has very good mechanical properties and superior corrosion and wear resistance, making it suitable for dental implants. Meanwhile, it could satisfy the increasing esthetic demands and metal-free requirement from many dental patients [45]. Besides, it is also revealed by in vitro and in vivo clinical studies that the biocompatibility and osseointegration of zirconia implants are superior when compared to the standard titanium implants [47].

Ebert et al. [48] adopted the direct inkjet printing method to make the zirconia dental prostheses. A zirconia suspension was synthesized with 27 vol.% solid part, by which specimens with a characteristic strength of 763 MPa, and a mean fracture toughness of  $6.7 \text{ MPa m}^{1/2}$  were achieved. It was indicated that this technique could be used to produce all-ceramic dental restorations with high accuracy at low cost, as well as minimal material consumption. Christian et al. [49] used SLM to fabricate  $\text{Al}_2\text{O}_3$ - $\text{ZrO}_2$  ceramic specimens. With a high density and crack-free feature, the manufactured parts exhibited fine-grained nano-sized microstructures and a flexural strength of

over 500 MPa, which could enable many medical applications such as dental restorations. However, preheating of the powders at 400 °C was required and the surface quality was poor. Later, Silva et al. [50] also fabricated the dental prostheses by an AM method, during which the alumina or Y-TZP were blended into a 0.8% aqueous solution of ammonium polyacrylate in a ratio of approximately 1:1 solid:liquid. In order to fabricate the zirconia dental implants, Lee et al. [51] developed a 3D slurry printing system (3DSP) and used a two-stage sintering process. The zirconia dental implant was successfully fabricated using this 3DSP system and the sintered parts have an average flexural strength and micro-hardness of 539.1 MPa and 1556 HV, respectively. Meanwhile, Chartier et al. [52] reported some achievements in the production of ceramics using photopolymerization technology, in which zirconia powder was one of the selected powders. The application of stereolithography was also demonstrated for healthcare and jewelry applications. Besides, 3D  $\text{ZrO}_2$  scaffolds have also been fabricated for biological engineering by direct write printing method, which provide potential application of in tissue engineering [53]. Lian et al. [54] adopted the mask projection stereolithography to customize the manufacturing of complex zirconia crown bridges, and obtained higher bending strength (after sintering) compared with human dentin. In this study, a three-part support structure was employed to ensure the dimensional accuracy during fabrication. Recently, Osman et al. [55] employed digital light processing (DLP) technique to print a custom designed zirconia implant. It was shown that the DLP technique could print customized zirconia dental implants with sufficient dimensional accuracy, as well as flexure mechanical strength close to those of conventionally produced ceramics. Fig. 2 shows the SEM images of the printed implants, which reveal several microcracks, porosities and interconnected pores ranging from 196 nm to 3.3  $\mu\text{m}$ . The differential shrinkage upon sintering induced by evaporation of solvent in the polymer loaded ceramic slurry on the exposed surface may lead to the observed cracks and porosities. Besides, the flaws may also be generated by insufficient amount of ceramic particles in the dispersion or the type of resin used. To achieve ceramic parts that are free of cracks and porosities, techniques such as systematic optimization of the 3D-printing process parameters and extra densification step following the completion of printing process are necessary.

## 2.3. Other applications

Other applications of 3D printed zirconia ceramics include fuel cells [56], electromagnetic BandGap antenna [57], electromechanical sensors [58], living supplies [51] owing to their high ionic conductivity, thermal and chemical stability, and mechanical strength. For example, Delhote et al. [57] designed and manufactured a woodpile-type photonic crystal for advanced millimeter wave applications based on 3D ceramic SLA process. The crystal was manufactured in one monolithic piece with zirconia, see Fig. 3a, and by which the sizes, shape and location of the waveguide could be optimized to maximize its bandwidth, as well as the match with the feeding waveguides. Such devices could provide a bandgap larger than 30%. Meanwhile, a 20% bandwidth was demonstrated at around 26 GHz with a return loss inferior to  $-10 \text{ dB}$ ,

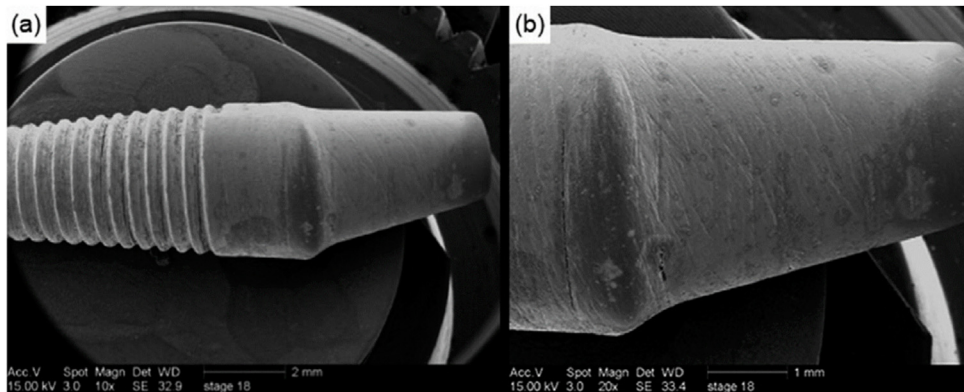


**Fig. 2 – SEM micrographs of the 3D printed zirconia dental implant. (a) Mag 10x, (b) mag 20x [55].**

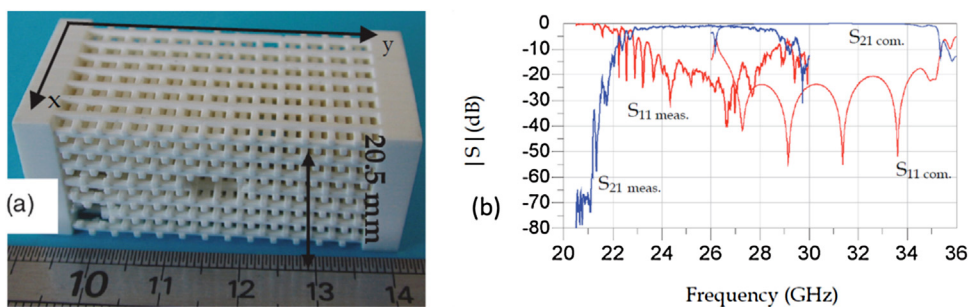


**Fig. 3 – The millimeter wave application of 3D printed zirconia ceramic. (a) Fabricated woodpile with zirconia based on ceramic SLA. (b) Scattering parameters of the waveguide located in the woodpile obtained from theoretical and experimental methods [57].**

as shown in Fig. 3b. When the reflexion parameter ( $S_{11}$ ) and transmission parameter ( $S_{21}$ ) reached the desired values, the waveguide was shown to be effectively capable of guiding electromagnetic waves (around 26 GHz in their example).

By using inkjet printing, Farandos et al. [59] obtained the electrochemical reactor cell: Ni-( $Y_2O_3$ )<sub>0.08</sub>( $ZrO_2$ )<sub>0.92</sub> (YSZ) | YSZ | YSZ-La<sub>0.8</sub>Sr<sub>0.2</sub>MnO<sub>3</sub> (LSM) | LSM, in which the parts were named based on the employed material systems in which the Ni-YSZ acts as the supporting substrate, YSZ acts as the electrolyte, YSZ-LSM acts as the electrode, and LSM acts as the current collection layer. The first step is to formulate the printable and stable colloidal dispersion of LSM-YSZ ink, and then the cell was formed by printing this LSM-YSZ ink sequentially onto an inkjet-printed YSZ electrolyte. The YSZ was sintered to a Ni-YSZ substrate in advance. These inkjet-printed YSZ-LSM electrodes have good performance exceeding those fabricated by conventional powder mixing processes. Fig. 4 shows the electrochemical properties of the reactors under dry H<sub>2</sub> [59]. It was demonstrated that the electrodes sintered at 1100 °C generated consistently greater current densities and lower overall cell polarisations, due to a greater density of triple phase boundaries than for electrodes sintered at 1200 °C.

AM technologies have also bloomed in fabricating sensors due to their unprecedented advantages [60,61]. However, there are limited studies for adopting AM methods in the manufacturing of ceramic sensors, especially for zirconia ceramic based sensors. Jafari et al. [62] developed a novel AM system for solid freeform fabrication of multiple ceramic actuators

and sensors. By using four extruders, the multilayer lead zirconate titanate (PZT) sensor components, which are constituted by two types of piezoelectrically active materials (soft and hard PZT), were successfully fabricated, as shown in Fig. 5(a) and (b). The performance characterization results shown in Fig. 5(c) and (d) indicate no sign of delamination. With further improvement of the accuracy and precision of the system, great potential could be expected for the fabrication of functional parts. Due to the importance of sensing technology and the great benefits from the AM methods, more applications will be demonstrated for the AM of zirconia ceramic sensors.

### 3. Additive manufacturing of zirconia ceramics

#### 3.1. Selective laser sintering

SLS is one of the current mainstream AM technologies developed by Beaman and Deckard in the 1980s at the University of Texas [63]. It is essentially a powder bed fusion process, in which fresh powder layers are applied sequentially and each layer is sintered selectively by a laser beam according to a pre-determined path. The final parts are often obtained through appropriate post-processing. There are two different types of SLS process for ceramics manufacturing: indirect SLS (iSLS) and direct SLS (dSLS). In iSLS, ceramic powders are mixed

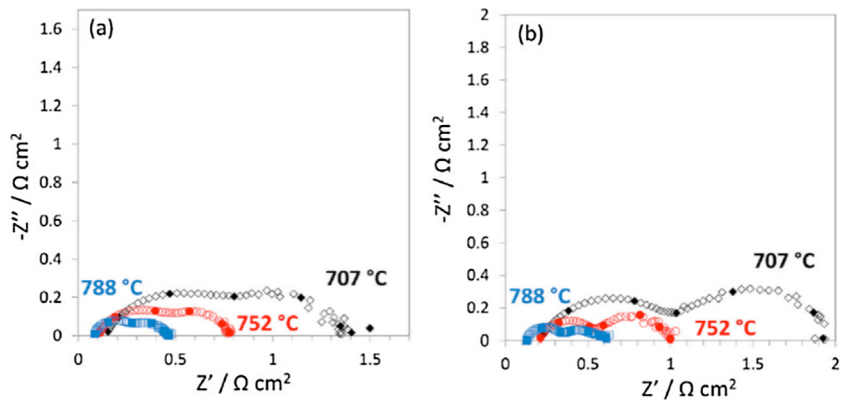


**Fig. 4 – Nyquist plots for Ni-YSZ | YSZ | YSZ-LSM | LSM cells at open circuit potential and operating with H<sub>2</sub> at different temperatures. YSZ-LSM electrode was sintered at (a) 1100 °C and (b) 1200 °C. Filled markers indicate decade intervals in frequency [59].**

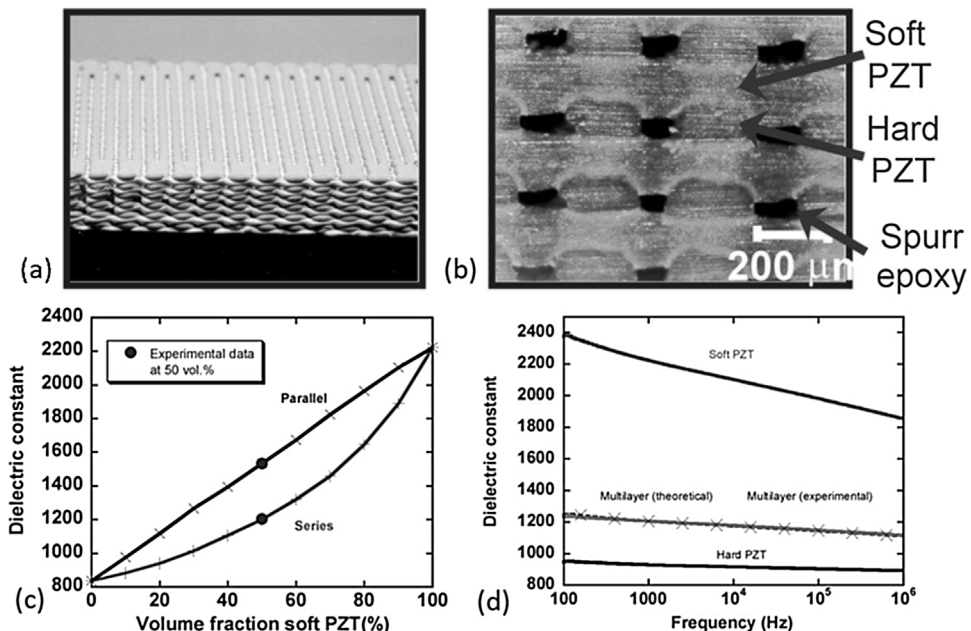


**Fig. 5 – The multilayer lead PZT piezoelectric sensor and its performance. (a) Green prototype, (b) sintered microstructure, (c) connectivity, and (d) frequency dependence of the dielectric constant [62].**

with a polymer binder and the melting of the binder by the scanning laser binds the ceramic particles together. In the follow-up debinding and sintering, the binder is removed and parts are densified [64]. In dSLS, no polymer binder is used and the ceramic particles are directly sintered by the laser beam. The interaction of the laser with the ceramic particles will cause the particles to bind together if the applied laser energy density is sufficiently high. In this case, no de-binding or furnace sintering is required afterwards [65]. For SLS, the usage of materials with high melting points such as zirconia ceramics is especially challenging. Typically, densification of these materials is a solid-state diffusion dominated process requiring high temperatures and long time to achieve acceptable densities. Another common issue is the thermal stresses induced by high heating and cooling rates. Because of the lim-

ited thermal shock resistance of ceramic materials, thermal stresses during SLS would lead to crack formation in sintered parts [66]. In order to reduce the crack and increase the density, efforts have been made through improving the powder characteristics and optimizing laser processing parameters.

### 3.1.1. Powder characteristics

Powder preparation in SLS remains the critical step of such a technique [67]. Generally, the higher the bulk density of the powder bed, the higher the density of the ceramic that can be achieved. Commercial powders have been studied and optimized in terms of morphology and particle size distribution in order to get a perfect powder layer. The earliest work was done by Gureev et al. [68] and Bertrand et al. [35], and both prepared ceramic parts containing zirconia powder for dSLS.

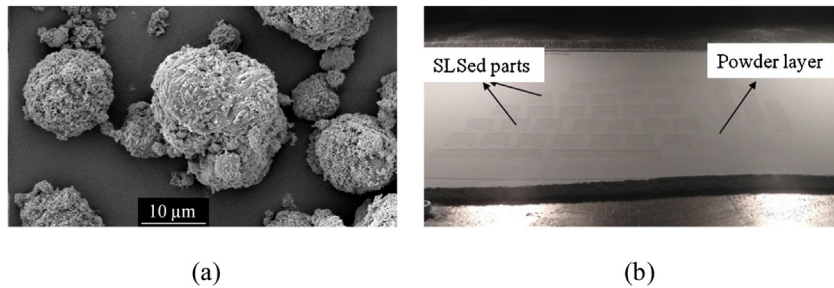


**Fig. 6 – (a)** SEM micrograph of PP-30 vol.% ZrO<sub>2</sub> microsphere powder produced by TIPS. **(b)** Roller deposited composite powder bed containing some SLS parts [72].

It was found that the density of the powder bed was a function of the size and shape of the powder and had a significant effect on the SLS process. The density of the powder layer could also be increased by colloidal techniques like slurry deposition by doctor blading [69,70] or spray deposition [71].

Besides the modulation of powder geometry, blending with another low melting point compound, e.g., polymer binder, could also be used to promote liquid phase sintering in the laser process and ultimately increase the ceramic density [72–74]. For example, by using thermally induced phase separation (TIPS), a spherical polypropylene (PP)-zirconia composite powder was produced by Shahzad et al. [72] for iSLS. The obtained composite particles are spherical, see Fig. 6a, with a wide size distribution in the 5–150 μm range. It was found that the powder bed can be preheated in a temperature region that is wide enough to avoid distortion of the parts induced by polymer crystallization during the SLS process. Besides, the powders showed a good flowability and uniform powder layers could be roller deposited, as shown in Fig. 6b. In addition, the compounds could also be used for assisting laser energy absorption. By adding a small portion of graphite to the YSZ powder, through simple mechanical blending, efficient energy transfer could be achieved between laser beam and powder bed, which is important for manufacturing dense YSZ parts [75]. It was demonstrated that YSZ parts with relative density of 96.5% could be obtained by this compound, outperforming other methods.

### 3.1.2. Optimization of laser parameters

Because different zirconia materials have different sintering temperatures [76], the laser parameters, such as laser power, scan speed, and scan spacing, should be designed according to the individual material types. Moreover, for a special material, the optimized process parameters should be adopted to obtain a dense ceramic part with fewer cracks. Fig. 7 shows the influence of laser power and scan velocity on the surface roughness, which clearly indicates that the roughness decreases with the decrease of laser power and increase of scan velocity. It was also pointed out that the strength of the parts would decrease in the same way. As a result, it was reported that for the parameter pairs in the lower right side, the parts could not be built completely, as well as the parts in the upper left side [69].

Researchers have also tried to overcome the problem of poor densification of direct laser sintered ceramics by

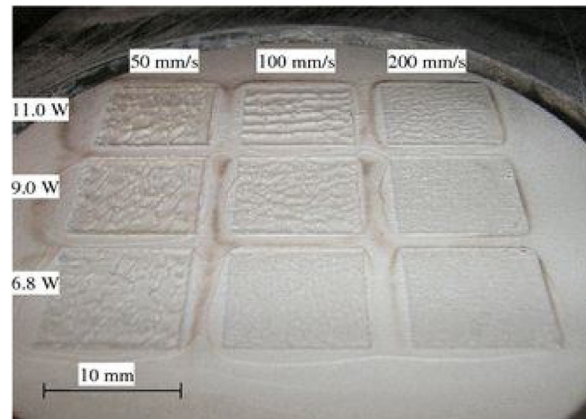


**Fig. 7 – Influence laser power and scan velocity on the morphology of zirconia part [69].**

combining the SLS process with other techniques such as self-propagating high-temperature synthesis (SHS) and ultrasonic vibration. For instance, Slocombe et al. [77] used the high exothermic redox-reaction of TiO<sub>2</sub>, Al and C to synthesize TiC-Al<sub>2</sub>O<sub>3</sub> composite ceramic. The raw materials were mixed together in powder form and placed onto the build platform of the SLS apparatus. Activation energy for the SHS reaction was induced by the laser. Besides, by introducing ultrasonic vibration to the AM process, the microstructure of ZrO<sub>2</sub>-Al<sub>2</sub>O<sub>3</sub> could be refined and uniformized, and compressive residual stress would be induced. Based on the ultrasonic-assisted LENS, the Al<sub>2</sub>O<sub>3</sub>-ZrO<sub>2</sub> ceramic parts could be manufactured with an average eutectic spacing of 70 nm and fracture toughness up to  $7.67 \pm 0.2 \text{ MPa m}^{1/2}$  [58]. The introduction of ultrasonic vibration helped to reduce grain size and improve microhardness, wear resistance, and compressive properties. Note that the attempts of combining the SLS process with other techniques for fabrication of zirconia ceramics are still limited, but their potentials appear to be promising, and thus more efforts should be made.

### 3.2. Laser melting of zirconia ceramics

Laser melting based zirconia ceramic AM technologies mainly include SLM and DED (namely, directed energy deposition), in which SLM dominates. SLM produces products in almost the same way as the direct SLS except that it is a one-step pow-

der bed fusion with full melting of materials. Thus a much higher laser energy is used, and the final structure is obtained without the usage of secondary low-melting binders or post-treatments. Recent research has demonstrated the possibility of using SLM to produce ceramic parts with high density and strength, as well as complex shape [78]. However, due to the intrinsic properties of zirconia ceramic such as low thermal shock resistance and high melting temperature, there are only a few studies on the selective laser complete melting of zirconia ceramic material. For instance, Shishkovsky et al. [79] demonstrated the fabrication of zirconia parts using SLM, while defects such as cracks and large open pores were observed in the parts. Bertrand et al. [35] fabricated zirconia parts using pure  $ZrO_2-Y_2O_3$  powder based on SLM, while the density of the products is low (56%).

To address the issue of low density in melting based AM technologies, limited successes have been reported in literature. By using laser-engineered net shaping (LENS), Niu et al. [80] prepared fully dense simple shaped  $Al_2O_3-YSZ$  parts with fine-grained microstructure. Nearly 100% density of  $ZrO_2/Al_2O_3$  parts was fabricated by Wilkes et al. [36] by completely melting  $ZrO_2/Al_2O_3$  powder mixtures using a focused laser beam. However, surface quality and dimensional accuracy remained unsatisfactory. In particular, it was found that the high thermal gradient induced cracks. Also, optimization of the laser parameters had little effect on mitigating such issues induced by thermal gradient, while preheating the ceramic powder bed was demonstrated to be more effective.

There are many benefits to pre-heat ceramic powders before the SLM process. Preheating of the ceramic powder at high temperature seems to be the most effective method of reducing cracks during SLM process. For instance, Liu et al. [81] found that the orderly cracks were transformed into disordered little cracks by the high-temperature preheating. When the preheating temperature increases, the most obvious improvement is in the distribution and morphology of cracks of  $ZrO_2$ -7 wt%  $Y_2O_3$  material, as shown in Fig. 8. Vertical cracks became disordered and short, and the cracks was not connected between the adjacent layers in the same scanning position. It is because that the high-temperature preheating can lower the SLM laser input energy, under which the cracks will not connect and propagate between the adjacent layers. Preheating promotes the homogenization of the energy distribution as well. Wilkes et al. [36] also stated that the employment of high-temperature preheating could prevent the possible crack formation during the build-up process of SLM. Net-shaped  $Al_2O_3/ZrO_2$  ceramic specimens with fine-grained microstructures, and outstanding mechanical and thermal properties were fabricated. By using preheating, other ceramic parts, such as the  $Al_2O_3/ZrO_2$  directionally solidified eutectic ceramics [82] and  $Al_2O_3/GdAlO_3/ZrO_2$  ternary eutectic [83] ceramics, have also been successfully obtained in a one-step SLM process with suppressed crack formation. Therefore, preheating processes could become a major consideration for the SLM processing of zirconia ceramics, and more research is called for in this regard.

It was also found that preheating the powder also has an important effect on the relative density of materials [81]. When preheated to 1500, 2000 and 2500 °C, the relative density of the yttria-stabilized zirconia made by mixing fine powder

(9–22.5  $\mu m$ , 20 wt%) and coarse powder (22.5–45  $\mu m$ , 80 wt%) increased from 84% (without preheating) to 90–91%. The crystal structure of the specimen with preheating was mostly tetragonal. That is because the room-temperature crystals for the zirconia powder include a mixture of zirconia polymorphs (monoclinic, tetragonal and cubic), among which the monoclinic structure would be transformed into tetragonal and cubic crystals during heating. The high cooling rate can conserve the high-temperature phases (tetragonal and cubic crystal) at room temperature. Besides, the laser melting process could promote the diffusion of yttria, which facilitates the formation of high-temperature phases. It was also demonstrated that the tetragonal crystal would become more apparent with the increase of preheating temperature.

In addition, the preheating process could also assist the enhancement of mechanical properties for the as-obtained objects. For instance, by using a high-temperature preheating of above 1600 °C during the SLM process, Hagedorn et al. [49] obtained parts with a fine grained microstructure and flexural strengths of above 500 MPa. They attributed the outstanding properties to the inhibited crack formation by the preheating process. Besides, Liu et al. [82] demonstrated that an assistant heating laser 3D printing method could successfully manufactured  $Al_2O_3/ZrO_2$  eutectic samples with suppressed formation of cracks. By optimizing the solidification parameters, it was shown that the average hardness obtained on the transverse section and the longitudinal section are 16.0 and 16.7 GPa, respectively, and the averaged fracture toughness values are 4.5 and 3.8 MPa  $m^{1/2}$  on the transverse section and the longitudinal section, respectively. However, the results indicated that the scanning rate hardly influences the mechanical properties.

### 3.3. SLA of zirconia ceramics

For SLA, the surface of liquid photosensitive resin is scanned by a light source, and a thin layer of a certain thickness can be formed for each scanning. These layers are then stacked and cured together to form the 3D part. This process is featured by high dimensional accuracy and surface quality, as well as the capability to produce complicated structure models [84]. Meanwhile, SLA does not require a high-energy laser beam. These features enable SLA to be one of the most important and popular AM technologies for fabrication of zirconia ceramics [85–87]. There are some distinct features associated with SLA of ceramics. For instance, the ceramic resins should have a low viscosity less than 3000 cps, and most ceramic resins can only have a loading less than 40 vol% [88,89]. Meanwhile, it is difficult to achieve ceramic 3D-printed objects with good mechanical and functional properties. In this section, we will address these challenges in SLA of zirconia ceramics based on the general steps including the preparation of raw materials and slurry, light curing, debinding and sintering. Meanwhile, digital light processing (DLP) technology, which could be categorized into SLA, has the advantage of improved printing rate due to the surface curing feature. Therefore, DLP should receive more research attention in the future and detailed discussion is put on this technology in the last part of the section.

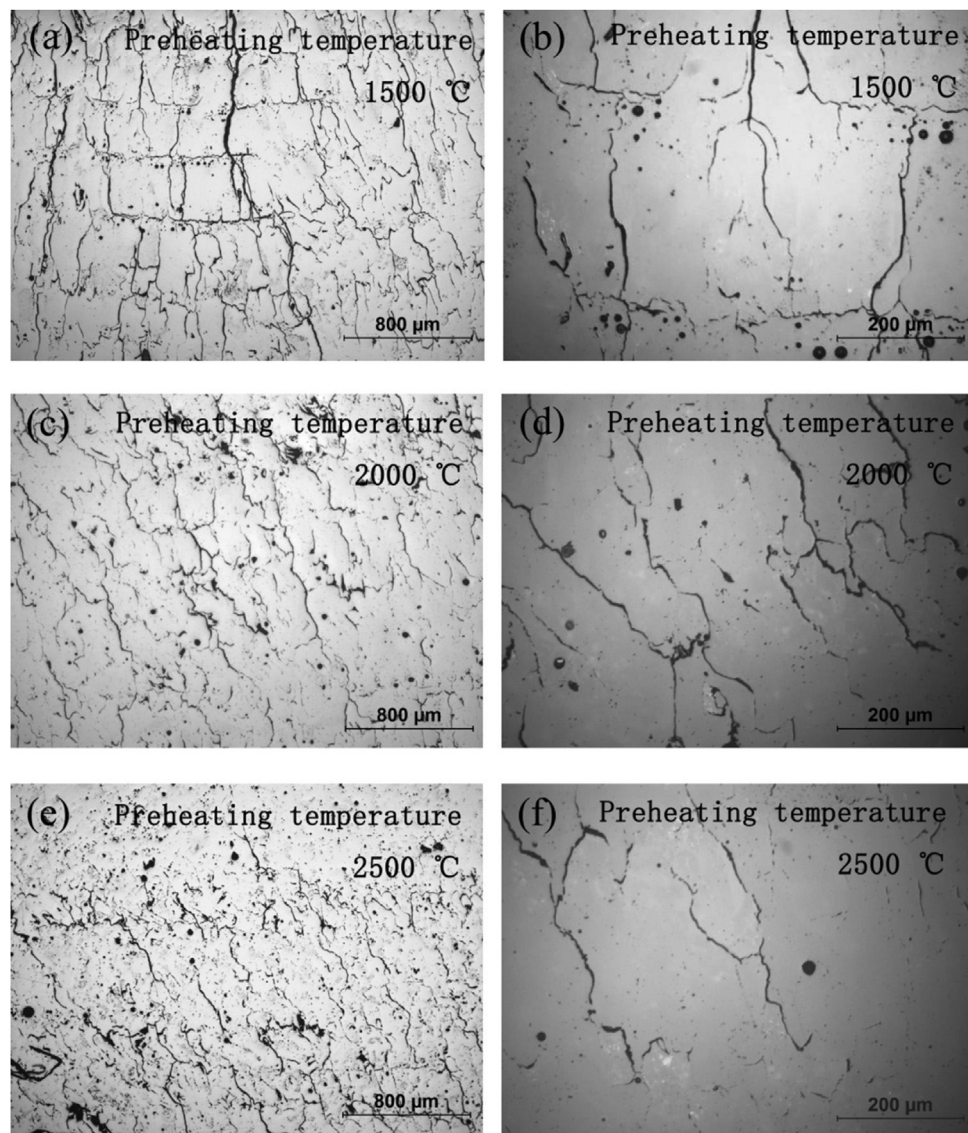


**Fig. 8 – Microstructure of  $\text{ZrO}_2\text{-Y}_2\text{O}_3$  specimens made at 60 W and different preheating temperatures ((a) and (b)) 1500 °C, ((c) and (d)) 2000 °C, ((e) and (f)) 2500 °C [81].**

### 3.3.1. Raw materials and slurry preparation

Formulating ceramic suspension is the first step in SLA, and the selection of the ceramic suspension is mainly determined by two properties, namely, the light adsorption and rheology. To produce a zirconia part with free-defect and high-performance, photosensitive suspension with a high solid loading, low viscosity and homogeneous dispersion is necessary. It was reported that a solid loading must be above 40% to avoid any defect after debinding and sintering for the SLA of ceramic [90,91]. However, the viscosity of the ceramic suspension will also increase with the solid content, which is unfavorable for achieving high homogeneous microstructure. When the solid content exceeds 60 wt%, the viscosity would increase exponentially [90,92], which is attributed to the reduced free water molecules for the high solid content. In order to maintain the rheological properties, repulsive forces should be induced, e.g., by adding steric dispersants [93]. By adsorbing onto the particle surface in the solution, disper-

sant could introduce steric repulsion effects to prevent particle agglomeration through its long chain structure, leading to reduction the viscosity of the suspension [94,95]. For example, Sun et al. [91] fabricated a  $\text{ZrO}_2$  part from the surface treated suspension with a solid loading of 42 vol%. However, the continuous increase of dispersant content would lead to the bridging between the long chains, resulting in an increase in the viscosity of the suspension [39]. Therefore, a proper content of dispersant should be kept. Generally, the solid loading is lower than 50 vol%, which usually results in  $\text{ZrO}_2$  parts with low density, high shrinkage rate and defect [85,91,96,97]. Recently, a high loading (55 vol%) photosensitive  $\text{ZrO}_2$  suspension was prepared by Zhang et al. [98], and this opened up new possibility for manufacturing high performance  $\text{ZrO}_2$  parts by SLA.

Another factor is the homogeneity of the dispersion. A homogeneous dispersion of ceramic powders in the SLA suspension is beneficial for enhancing the curing performance of

the suspension, as well as the shaping and preparation of the green body [99]. To improve the homogeneity of the ceramic suspension, ultrasonic agitation and ball-milling steps are often used. By using the solution mixing technique (SM), Faes et al. [100] obtained a homogenous dispersion containing up to 55% vol concentration of zirconia, dispersed into XC11122 UV resin. The dispersion based on ceramic powders and UV-resin was selectively deposited using a syringe, followed by curing using a power-LED array. The influence of dispersion homogeneity, rheology, and printability on the properties of final products was investigated, and a sample with 92.1% density and high strength was achieved. Li et al. [101] extensively investigated the slurry properties of zirconia dispersion by using 12 different dispersants. Rheological measurements showed that among the 12 dispersants, the dispersant made of a copolymer with filler affinic groups was particularly effective. With 3.5 wt% of the particular dispersant, 42 vol% ZrO<sub>2</sub> suspension was successfully prepared with a viscosity lower than the threshold viscosity value for stereolithography. Wu et al. [102] combined the traditional methods of liquid precursor infiltration with in situ precipitation with stereolithography-based 3D printing for the fabrication of Al<sub>2</sub>O<sub>3</sub>–ZrO<sub>2</sub> ceramics, which greatly ensure the homogeneous distribution of ZrO<sub>2</sub> particle in the alumina matrix.

For SLA of ceramics, the attenuating of UV light by scattering could greatly reduce the photopolymerization reaction. ZrO<sub>2</sub> has a large refractive index, which could result in more UV light to be absorbed by the ceramic filler material, leading to reduced curing depth [103]. Therefore, a ceramic filler with lower refractive index such as Al<sub>2</sub>O<sub>3</sub> is expected. Introducing Al<sub>2</sub>O<sub>3</sub> into ZrO<sub>2</sub> could alleviate this phenomenon, while other techniques are highly expected for further addressing this challenge.

### 3.3.2. Light curing

During curing, the monomers undergo a radical photopolymerization, or an ionic photopolymerization [104]. The radical polymerization is sensitive toward the diffusion of oxygen from the air into the photocuring liquid, which is disadvantageous. For ionic photopolymerization, it does not stop immediately after the end of the light exposure [66]. Heat is generated during both of the photopolymerization reactions, leading to a curl distortion of the photocured structure or to an increase in shrinkage when sintering the photocured structure. Construction errors in the finished structure can be prevented by considering the combined effect from the released light energy and the evoked reaction heat.

Multiple cured tracks have to be overlapped with each other in order to generate a uniform connection between the numerous curing tracks. Corcione et al. [105] indicated that the temperature rise within the photosensitized liquid is proportional to the applied energy dose during an exposure, the distance from the center of the light beam, as well as the inverse of the scanning speed. Wang et al. [106] stated that in the area exposed to the blue light, the photopolymer reacted with the light and bonded with neighboring structural particles, which caused a photopolymerization effect and solidified the area, resulting in the formation of the green part. The area without exposure to blue light remained as a gel-like layer, uncured and acting as the supporting material. This process

was repeated until the last layer was provided by the computer.

### 3.3.3. Debinding and sintering

After the formation of the zirconia ceramic green part, significant quantities of organic resin (binder) still remain. Thus, a debinding process must be performed to remove these resins. During the debinding process, efforts should be made to avoid cracks. The debinding behavior depends on several factors such as resin composition, solid loading, and component geometry. To obtain pure zirconia ceramic brown bodies with inhibited defects, a two-step debinding process, which constitutes a vacuum debinding and a follow-up air debinding, was proposed by He et al. [96]. The vacuum debinding could reduce the decomposition rate of organic compounds within the green bodies, thus the occurrence of defects such as cracks and bubbles was reduced as well. Air debinding was then performed to remove the carbon residues. Similarly, Wu et al. [93] adopted a two-step debinding process to remove the binders in the Al<sub>2</sub>O<sub>3</sub>–ZrO<sub>2</sub> ceramic compact. Firstly, the samples were heated at 600 °C for 3 h in vacuum with a heating rate of 1 °C/min. After vacuum debinding, the samples were heated at 1000 °C for 30 min in air with a heating rate of 5 °C/min.

Sintering is the last stage where pores between the particles are eliminated. It is needed to create a fully dense components and well controlled microstructure to achieve a zirconia part with high-performance. The densification and strength of sintered zirconia depend on sintering temperature and temperature gradient. The heating process should be performed very slowly to allow the entire green part to absorb and dissipate energy uniformly. Internal cracks could be induced by rapid absorption and dissipation of heat, leading to possible breakage of the green parts [106]. The representative sintering parameters are summarized as follows. In the work of Wu et al. [93], the sintering temperature of alumina/zirconia was varied at 1500, 1550, 1600, and 1650 °C, and the holding time was 1 h by using a muffle furnace. The highest relative density achieved was over 95%, and the maximum Vickers hardness and fracture toughness were 17.6 GPa with the sintering temperature of 1550 °C and 5.2 MPa m<sup>1/2</sup> with the sintering temperature of 1650 °C, respectively. By setting the post-sintering temperature at 1500 °C with a holding time of 1 h and heating rate of 3.75 °C/min, He et al. [96] obtained the relative density of 97.14%, Vickers hardness of 13.0597 GPa, and fracture toughness of 6.0380 MPa m<sup>1/2</sup> for ZrO<sub>2</sub> parts. Significant shrinkage with a maximum value of 35.26% after sintering was achieved. Wang et al. [106] attempted sintering at high temperatures (up to 1600 °C), and the zirconia green parts were initially heated from 40 to 350 °C in 1 h 30 min at a rate of 3.4 °C/min. The obtained ceramic parts had a mean density of 99.45% with a standard deviation of 0.35%, average flexural strength of 731.11 MPa, and average surface roughness of 0.735 μm. In the research of Xing et al. [107], the ZrO<sub>2</sub> green parts were heated to 500 °C at 0.2 °C/min and retained for 18 h for the binder to be burned out under a nitrogen gas atmosphere. The samples were subsequently heated at 7 °C/min to 1450 °C and retained for 2 h under the nitrogen atmosphere. Up to 99.3% density of ZrO<sub>2</sub> was obtained. The flexural strength, fracture toughness, and hardness of ZrO<sub>2</sub> ceramics reached 1154 ± 182 MPa, 6.37 ± 0.25 MPa m<sup>1/2</sup>,

and  $13.90 \pm 0.62$  GPa, respectively. The surface roughness of the horizontal surface was below  $0.41\text{ }\mu\text{m}$ , while it reached  $1.07\text{ }\mu\text{m}$  on the vertical surface. Liu et al. [108] claimed that for the SLA printed  $\text{ZrO}_2\text{-Al}_2\text{O}_3$  composite ceramics, the density, hardness and fracture toughness could reach  $3.75\text{ g/cm}^3$ ,  $14.1\text{ GPa}$ , and  $4.05\text{ MPa m}^{1/2}$ , respectively, under the condition of  $1500^\circ\text{C}$  sintering temperature and 60 min holding time. With the further increase of sintering temperature and holding time, the actual density would gradually increase and then reach a saturation level. Besides, the influence of residual monomer on cracking for the fabrication of zirconia ceramic is important. It has been reported that the cracking in ceramic fabricated by SLA could be avoided by changing the build style to eliminate the residual monomer [109], based on which more efforts are called for to control the cracking behavior in the SLA of zirconia ceramics.

### 3.3.4. Digital light processing

For DLP technology, a digital micromirror device (DMD) is used to directly project the image into the whole area to realize surface curing [110,111]. As such, the scanning can be cured in a single layer, which greatly improves the printing rate, and the accuracy mainly depends on the resolution of the DMD device. Digital light processing system was developed for the fabrication of complex technical ceramics, requiring high levels of detail and accuracy. The parts can be built using a bottom-up or top-down configuration by DLP. In a bottom-up set-up, a part is built not fully immersed in the liquid feedstock, but mounted upside down on the building platform and dipped in a thin slurry layer deposited on a glass plate. A striking advantage of this strategy, compared with the top-down orientation, is the small amount of slurry required for building the part [112]. Bottom-up printers are also generally less expensive, but the top-down printers have the advantage of executing larger designs.

The DLP-system used in the study of Mitteramskogler et al. [23] created a ceramic green part by stacking up layers of a photo-curable resin with a solid loading of around 45 vol.% zirconia. Light scattering within the ceramic filled slurry caused a certain amount of widening of dimensions in the final geometry, and that this overgrowth was both sensitive regarding overall exposure area and exposure time. Softstart light curing strategies and higher values for depth of cue were preferred for the successful thermal processing of a 3D-printed green part.

One of the critical steps in ceramics stereolithography is the preparation of a photo-curable slurry with properties that fulfill specific requirements, such as having a low viscosity, high solids loading and appropriate curing characteristics. Komisarenko et al. [113] studied the rheological and curing behavior of slurries with different acrylic monomers and ceramic fillers in DLP. New formulations based on mono- and tri-functional acrylic monomers revealed the following excellent rheological properties: The viscosity of the mono-/tri-acrylate-based slurry with 75 wt.% of zirconia was  $1.6\text{ Pa s}$  at  $30\text{ s}^{-1}$ . High precision 3Y-TZP strengthened  $\text{ZrO}_2$  ceramic parts with micro-pore network structures were successfully prepared by using DLP [114]. The highest relative density and flexural strength values were obtained at 96.40% and  $306.53 \pm 6.03\text{ MPa}$ , respectively, when the 3Y-TZP concentration was 7.5 vol.%.

### 3.4. Inkjet printing of zirconia ceramics

The 3D IJP ceramic manufacturing technology works by heating the nozzle to vaporize the ceramic ink in the capillary at the bottom of the nozzle in a very short time and form bubbles to expand rapidly. The bubble would expand to a critical value overcoming the surface tension of the ink, leading to ejection of the ink from the top of the nozzle capillary. The ceramic ink is drawn according to the data pre-modeled by the computer, and the layer is superimposed to realize the 3D ceramic parts. Inkjet printing is an economical AM technique with minimal material waste, high flexibility, and short lead time, which make it an excellent candidate process for the manufacturing of ceramic components [27,115,116]. The IJP procedure mainly includes ink preparation, printing, and sintering. The first demonstration of IJP to print ceramic parts was made by Blazdell et al. [117] in 1995, for which the  $\text{ZrO}_2$  and  $\text{TiO}_2$  inks were used. Since then, more efforts have been made to achieve high-performance zirconia ceramic products by IJP methods [118–121], among which the focus is on the investigation of the ink characteristics and the coffee staining effect during the deposition of particle-loaded drops.

#### 3.4.1. Ink characteristics

For IJP, the dimensional resolution is affected by the ink parameters such as solid content, particle size and viscosity [122,123]. Therefore, preparing suitable zirconia inks that ensure colloidal stability and printability for the IJP process is a critical first step. Normally, the jetting behavior of the inkjet inks can be represented by the dimensionless Ohnesorge number ( $\text{Oh}$ ), which can be calculated using the physical ink properties:

$$\text{Oh}^{-1} = \frac{(\sigma \cdot \rho \cdot \alpha)^{1/2}}{\eta} \quad (1)$$

where  $\sigma$  is the surface tension,  $\rho$  is the density,  $\alpha$  is a characteristic length (the nozzle radius), and  $\eta$  is the viscosity of the ink. The suitable region for stable jetting is defined as  $1 < \text{Oh}^{-1} < 10$  [124–127].

The IJP ceramic parts are typically prepared based on two types of inks: wax-based inks, which are deposited in hot melted state and solidified on a cold substrate [128,129], and ceramic suspensions, which are dried through evaporation of the liquid [127]. Gingter et al. [130] developed aqueous inks based on fine zirconia powder (3Y-TZP) with a solid content of 21 vol% for a direct inkjet printing (DIP) system. By optimizing the solids content, surface tension and viscosity of the inks, as well as good performance zirconia parts with up to 97.5% of the theoretical density could be obtained. The microstructure was homogeneous, and no lamination or other process-related defects were detected. The dynamic viscosity of optimized 3Y-TZP was  $4.8\text{ MPa s}$  and the surface tension was determined to be  $50.3\text{ mN m}^{-1}$ . Farandos et al. [59] formulated a printable and stable colloidal dispersion of  $\text{La}_{0.8}\text{Sr}_{0.2}\text{MnO}_3$  (LSM)-( $\text{Y}_2\text{O}_3$ ) $0.08$ ( $\text{ZrO}_2$ ) $0.92$  (YSZ) ink to sequentially print onto an inkjet printed YSZ electrolyte sintered to a Ni-YSZ substrate to form the cell. The viscosity, surface tension and  $\text{Oh}^{-1}$  numbers for the LSM-YSZ ink were  $8.34\text{ MPa s}$ ,  $19.6\text{ mN m}^{-1}$ , and 2.3, respectively. The inkjet-printed cells showed a peak fuel

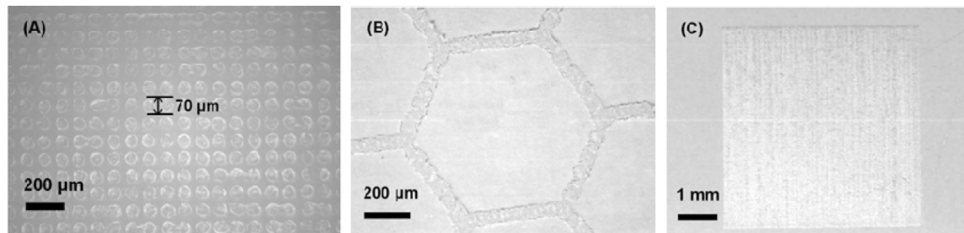


**Fig. 9 – (a) separated splats, (b) honeycomb pattern, and (c) continuous squared layer obtained using the nano-inks transferred from the continuous hydrothermal synthesis [132].**

cell power density of  $0.69 \text{ W cm}^{-2}$ , cell potential difference of  $1.5 \text{ V}$  and electrolysis current density of  $3.3 \text{ A cm}^{-2}$ , which outperformed those fabricated by conventional methods. Besides, aqueous inks of 3Y-TZP and carbon were developed and characterized for the DIP method by Özkol et al. [124]. The viscosity values of the ceramic and supportive inks were determined to be around 15 and  $4 \text{ MPa s}$ , respectively. The surface tension of the ceramic and supportive inks was measured as around 42 and  $38 \text{ mN m}^{-1}$ , respectively. By using these inks, ceramic parts were obtained with a relative density of  $>96\%$  of the theoretical density and a flexure strength of around  $843 \text{ MPa}$ . Wang et al. [131] prepared suspensions of  $\text{Pb}(\text{Zr}_{0.53}\text{Ti}_{0.47})\text{O}_3$  (PZT)-5H powders, with solid contents up to 40 vol% in a paraffin oil/wax medium using a mixed polyester and amine dispersant system. Sufficient suspension stability for printing requires a sub-micron particle distribution, which could only be achieved by attrition milling the as-received powder. Ceramic parts with full density, porosity less than 1% and without significant distortion were fabricated. In Li et al.'s work [53], the water-based  $\text{ZrO}_2$  ink with a solid content of 70 wt% was prepared for the direct write printing of 3D  $\text{ZrO}_2$  scaffolds. High precise control of the internal architecture could be achieved, which has high potential to be applied in biomaterials and tissue engineering scaffolds. To formulate finely dispersed nano-colloids for nano-inkjet, Rosa et al. [132] transferred the water dispersions of nanometric YSZ particles synthesized by continuous hydrothermal synthesis to the nano-inks. Additives were used for regulating the viscosity and surface tension. It was demonstrated that zirconia parts with high lateral and thickness resolutions could be fabricated (Fig. 9).

#### 3.4.2. Coffee staining

Although the quality of the zirconia parts could be improved by careful design of ink properties and extrusion parameters such as the extrusion rate and nozzle travel speed, as well as the distance between the nozzle and the previously deposited layers, major concerns (e.g., coffee effect) still remain. Coffee straining happens in the drying of as-printed patterns [133], during which the solid particles segregate from the center to the edge of the printed patterns [134]. This effect could generate unwanted defects in the printed structures.

Dou et al. [135] investigated coffee staining behavior of printed drops on a range of substrates including glass microscope slides, an epoxy resin and preprinted and dried  $\text{ZrO}_2$  powder layers. By adding 10 wt% PEG into the original ink, the coffee staining can be removed on solid substrates.

Using the modified ink, coffee staining was completely eliminated at room temperature ( $25^\circ\text{C}$ ). However, at temperatures above  $35^\circ\text{C}$  coffee staining was again observed, which can be explained by diffusion reducing the concentration gradients that drive Marangoni flow. When modified ink was printed onto a layer of dried ceramic powder, coffee staining was found at room temperature, which is attributed to the drops drying by the draining of fluid into the dried powder bed. With the addition of a fast drying agent, i.e., 50 vol% isopropyl alcohol, Friederich et al. [136] demonstrated the rapid increase of the ceramic ink viscosity after deposition and a completely suppressed coffee strain effect. Because significant differences exist between the mechanisms of coffee staining driven by evaporation and capillary draining [137], more appropriate models needed to be developed by incorporating evaporation, draining, Marangoni flows, and multicomponent solution for better understanding and elimination of coffee straining.

#### 3.5. Other AM techniques for zirconia ceramics

Besides the above-mentioned methods, some other AM techniques, such as binder jetting [138], 3D gel-printing [139], freeze-form extrusion [24,140], thermoplastic 3D printing [141,142], freeform extrusion [143], robocasting [144], direct inkjet printing [48,145], and extrusion-based photoreaction method [99,146] have also been adopted in the fabrication of zirconia components. For instance, a novel freeze-form extrusion fabrication (FEF) process was developed by Leu et al. [140] for the fabrication of 3D ceramic parts with functionally graded  $\text{Al}_2\text{O}_3$ - $\text{ZrO}_2$  materials. A triple-extruder FEF system working in a temperature under water's freezing point was designed with the capability of fabricating 3D parts with desired  $\text{Al}_2\text{O}_3$  and  $\text{ZrO}_2$  gradient (Fig. 10), which is useful for manufacturing functional materials. Also, Yu et al. [147] proposed an extrusion-based AM process for fabricating yttria-partially-stabilized zirconia ceramics with high relative density and superior mechanical properties. Relative density of 98.1% was achieved with a rapid cooling process and the mechanical properties were reported to be higher than those fabricated by binder jetting and SLS. Meanwhile, ceramic parts that have no cracks or large pores have mechanical properties close to those of conventionally produced ceramics. Such parts can be fabricated by optimizing the AM process parameters or performing extra densification steps after the AM process. In order to produce crack- and pore-free ceramics with AM, it is also advisable to incorporate colloidal processing techniques into the AM process [148,149]. Among these methods, binder

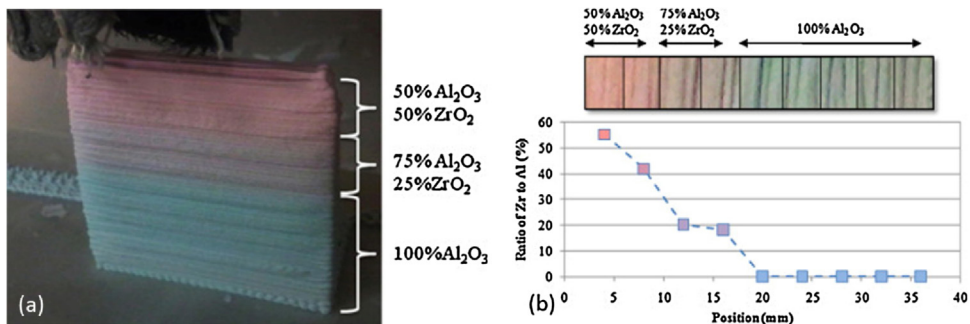


Fig. 10 – (a) An FEF prepared  $\text{Al}_2\text{O}_3/\text{ZrO}_2$  object with gradient  $\text{Al}_2\text{O}_3$  proportion and (b) the EDS intensity measurements [140].

jetting, fused deposition modeling, digital light processing and materials extrusion hold the highest potential for wide applications.

### 3.5.1. Binder jetting

Binder jetting is an additive manufacturing process in which powder particles are joined together by a selectively deposited liquid binding agent. An object is then formed by the bonding of layers of material. Binder jetting is unique in that it usually does not employ heat during the build process, which could avoid the generation of residual stresses in the parts commonly happening in other additive techniques that utilize a heat source. Additionally, the parts are supported by the loose powders in the job box during binder jetting, eliminating the need for a build plate. Moreover, the spreading speeds for binder jetting significantly outperform other processes. Binder jetting has the ability to print large ceramic parts and is often more cost-effective than other AM methods as well.

In work of Manogharan et al. [150], stabilized zirconia as electrolyte was explored by jet printing to produce porous structures to increase the effective surface area during surface-fluidic interface. Zhao et al. [138] used a 10 wt% zirconia nanoparticle suspension as the binder material in the printing liquid to print zirconia ceramic samples. The result showed that by increasing the binder content to the upper limit of investigation range, the relative density of the printed parts increased from 75.2% to 86.8% while linear shrinkage decreased from 22.3% to 10.6% after sintering.

### 3.5.2. Direct ink writing

In the direct ink writing (DIW) process, the ceramic suspension with a high solid loading are built up by moving nozzles to directly “write” the designed shape layer by layer until the part is complete. It is typically followed by debinding and sintering so that the part is free of organics. The technique was originally patented and developed by Cesarano at the Sandia National Laboratories in the USA under the name of “Robo-casting” [151]. DIW is widely used for patterning and selective deposition of different types of materials. It has the capability of forming high-resolution single and multiple layers, and allows the deposition of a variety of materials on both planers as well as conformal surfaces.

There are many factors affecting DIW finished products, such as the nozzle size, viscosity and density of the material, scanning speed, eject speed, sintering process, drying steps

and other parameters. Since the slurry is quickly dried in the air after being extruded from the nozzle, the ceramic slurry with a high solid content undergoes a transition from a pseudoplastic fluid to an expanding fluid and solidifies. An optimal deposition object can be obtained by controlled flocculation of a ceramic suspension to form a gel [152], and using gelling additives, polymeric binder and plasticizer [152].

The molding processes of binder jetting, IJP and DIW are similar, which consist of mixing ceramic powders with solvent and binder into a slurry, and extruding or injecting through a certain nozzle technology to form the desired ceramic body shape. After high temperature debinding and sintering, the required ceramic material components are obtained. In the work of Yu et al. [153], the extrusion-based approach was used to print high solid loading zirconia paste (60 vol.%), which was partially-stabilized (3 mol%  $\text{Y}_2\text{O}_3$  stabilized). After debinding and sintering, a high relative density of 98.1% was achieved, and the mechanical properties were claimed to be higher than those obtained by binder jetting and SLS.

The solid loading of ceramic suspension in DIW is generally higher than that of IJP, and the nozzles of DIW are required to be generally much larger than those of IJP nozzles owing to the higher viscosity of the materials used. The typical nozzle sizes of DIW are in the range of 100–1000  $\mu\text{m}$ , however, drying in air limits the minimum diameter of the printing nozzle to about 500  $\mu\text{m}$  to prevent clogging [148].

For DIW of  $\text{ZrO}_2$ , one of the key issues is to develop better  $\text{ZrO}_2$  inks with the ability to generate complex 3D structures with micro- and nano-scaled resolution and large span capability. Liao et al. [145] developed a novel avenue to tailor the rheological properties of concentrated zirconia colloidal inks for DIW by slightly changing the concentration of  $\text{NH}_4\text{PAA}$ . The prepared zirconia colloidal ink has good mechanical properties, which was then successfully used to fabricate 3D structures with fine integrity. Ebert et al. [48] synthesized a tailored zirconia-based ceramic suspension with 27 vol% solid content. Based on this suspension, zirconia dental parts with characteristic strength of 763 MPa, and fracture toughness of 6.7  $\text{MPa}/\text{m}^{1/2}$  was 3D-printed. The DIW of  $\text{ZrO}_2$  has many advantages, though many challenges still exist, and thus more research is called for in the near future.

### 3.5.3. Fused deposition modeling

In the fused deposition modeling (FDM) process, the ceramic-polymer stock material is fed into the printing head, heated

above the melting temperature of the polymer material, and then extruded from the nozzle. Three-dimensional components can be formed by controlling the movement of the Z-axis [146]. The shaped body is subjected to debinding and sintering to obtain the final ceramic part. FDM can be used for the production of dense single- and especially multi-material components.

In Scheithauer et al. [141], the droplet formation behavior of zirconia suspensions for T3DP (82 and 84 wt.%) was investigated. The droplet fusion factor (dff) is introduced to calculate the necessary distance between two droplets to form filament-like structures by fusion of adjacent droplets. For a dff between 56 and 66%, filaments could be produced with constant width, which does not increase too much compared to the diameter of single droplet. The deposition of suspension with a lower solid content results in wider filament for a small dff. The maximum width of the filament produced with a dff of 66% and higher is comparable for both suspensions.

Later on, Scheithauer et al. [142] obtained ceramic-based functionally graded materials by using the thermoplastic 3D printing. Different zirconia-based suspensions were prepared and used for the AM of single- and multi-material test components. All of the samples were sintered defect-free, and became a brick wall-like component consisting of dense (<1% porosity) and porous (approx. 5% porosity) zirconia areas.

Based on the above discussion, it is clear that each AM method has its own advantages and disadvantages for the zirconia ceramic fabrication. For example, although SLS has the advantages of support-free and wide range of material combinations, the ceramic parts usually have low resolution, poor surface finish and porous microstructures. SLM can produce fully dense homogeneous ceramic parts, while it is limited by the generation of defects. It is necessary to select the suitable fabrication method based on the specific application scenario, while it is difficult to develop a simple, scalable and controllable AM method to produce all zirconia parts with high-performance.

## 4. Challenges and opportunities

AM could bring about improved performance for complex material/structural or multi-objective design, which is unmatched by traditional preparation methods [154]. AM techniques are also able to reduce customization costs and lead time for individualized parts such as implant and prostheses [155]. However, the zirconia ceramic AM processes are not very mature, and many challenges need to be addressed, in which raw materials, process control, ceramic printer development and modeling as well as simulation stand out. Considerable research efforts ought to be made for the AM technology to become more competitive compared to the traditional fabrication technologies.

### 4.1. Difficulties in preparing raw materials

Material technology, which restricts the development of 3D printing to a certain extent, is one of the cores to 3D printing technology. For each AM technology, the feedstock must be provided in a form compatible with the process (e.g., powder,

sheet, wire, or liquid-based) [156]. Meanwhile, the materials should ensure the important in-service performance such as reduced porosity and improved surface finish, as well as enhanced strength and geometric accuracy. As for zirconia ceramics, currently the raw materials are present in the form of slurry, powder, or bulk solid as required by the type of AM method [78]. In general, the development of zirconia ceramic raw materials faces enormous difficulties. For instance, even though inkjet is considered as a major method of making dense ceramic samples [66], it still faces the issues of nozzle clogging, breaking and thinning of the printed filament [110,157]. To address these issues, efforts should be made to synthesize a stable suspension with controlled rheology, flowability, and good viscoelastic behavior. Besides, to relieve the crack formation during the SLS processing of ceramics, a binder with a lower melting temperature is often used [158]. During the SLS, the particle size distribution of ceramics is critical to the density, flowability, and shrinkage of the printed objects [159], which should receive important attention from SLS processing of zirconia. For the extrusion based methods, rheology of the raw ceramic materials is the main controlling factor [160]. Besides, the properties of the 3D printed parts are also affected by the particle size distribution and packing of particles in the paste, the liquid to solid ratio. In the SLA processing of zirconia ceramics, it is preferred to strike a balance between the particle size with the resultant light scattering properties [66]. This is because smaller particles generally lead to the increase of light scattering, which increases the width of curing track but decrease the penetration depth. However, it was demonstrated that the particle size distribution of ceramic powder in the paste has limited influence on the SLA technique when compared to the powder printing by SLS method [160].

### 4.2. Limitations of ceramic printing systems

Various 3D printers have been developed and become commercially available for each of the AM methods [161–163]. However, due to the inherent difficulties existing in ceramic manufacturing, especially for zirconia ceramic manufacturing, such as extreme hardness and brittleness, high melting point, and low expansion coefficient, only a handful of the printers could be used for zirconia printing [75]. Even for the available ceramic 3D printers, technical difficulties have been still existing which strongly restrict their capability of making zirconia ceramic components. For example, for the laser melting/sintering based ceramic AM methods, it is generally required that a preheating or working temperature higher than 1000 °C, which imposes high demand for the printers. For the SLA based ceramic AM methods, the printers have the fundamental problem that the non-trivial effect of light scattering would arise from the added ceramic particles. For the IJP based methods, many printers are prone to the possible corrosion of the jetting system by the ink, as well as the clogging and blockage of nozzles and capillaries. As such, equipment manufacturers are tasked to improve their existing ceramic 3D printers, and develop new ceramic 3D printers based on other AM processes.

Meanwhile, the existing ceramic 3D printers are also limited by the build size, high equipment cost, and low build rate.

Large ceramic objects are still not feasible when built using 3D printers. For instance, to our best knowledge, the largest build volume is claimed by the ExOne Exerial Industrial Binder Jetting system, at  $2200 \times 1200 \times 600$  mm. Meanwhile, the wide application of AM processed zirconia ceramic requires the fabrication of ceramic 3D printer with low cost, but this is still not the case with the current technology. The capability of mass-producing zirconia ceramic products is a key requirement for industry, but the build rate of existing ceramic 3D printers seems to be a bottleneck in many cases. For example, the theoretical maximum building rate for inkjet printing of ceramics is reported to be around  $1 \text{ cm}^3/\text{s}$  [116]. However, the practical building rate is usually much lower due to the consideration of object resolution. It thus calls for more advancements and innovations to develop new ceramic 3D printers with printing capability of large size, low cost and high speed.

#### 4.3. Deficiencies in existing AM processes

Though some commercially available AM systems capable of printing zirconia ceramics have been demonstrated, there exist various misalignments between the current AM ceramic capabilities and the performance requirement in applications. For the zirconia ceramic matrix composites by the current AM processes, various issues such as porosity, purity, defects and cracks commonly exist [148], which is hard to overcome within the existing AM framework. Meanwhile, the intrinsic features of the AM processes, e.g., staircase effect and lack of microstructural quality control, could significantly compromise the advantages of AM processing of zirconia ceramics [164,165]. For some of the available AM ceramic techniques, the need of post processes such as debinding and sintering would bring increased complexity and cost, as well as challenges, such as the limitation of feature thickness and distortion during the debinding/sintering [166]. Moreover, in the powder based AM techniques, it is expected to use finer ceramic particles for achieving higher sintering density. However, the lower flowability could be generated by the refined particles, which would negatively impact the benefits of AM zirconia ceramics [154]. What is more, the powder suspension based AM methods have limited ceramic content, resulting in lower density for the printed products.

#### 4.4. Lack of modeling and simulation efforts

Modeling and simulation are important to understand the underlying mechanism of the AM process for zirconia processing, as well as uncovering the dynamic phenomena such as microstructural and stress evolution which are otherwise hard to be captured by experimental methods. With such capability, the process parameters can be optimized and the mechanical properties can be ensured to reach the desired values. Some trials have been made in for AM processing of  $\text{ZrO}_2$ . For instance, finite element analysis (FEA) was performed to investigate the stress distributions inside the zirconia framework structure during the direct inkjet printing process. Various loading conditions were considered, and the maximum tensile stress on a zirconia dental framework would be  $\sim 340 \text{ MPa}$  under realistic clenching conditions [93]. The curing process can be more accurately described by involving the

Kubelka–Munk model in theoretical calculation [167–169]. The Kubelka–Munk model takes the changes in reflectance, transmittance and absorbance that arise when ceramic particles are added to the photocuring liquid into account. Recently, Tarabeux et al. [170] developed a numerical simulation model for predicting the curing behavior of ceramic in the SLA process. With the consideration of the UV-laser beam scattering phenomenon induced by the ceramic particles, the developed model could be successfully validated by experiment using a commercial photopolymerizable alumina paste. Meanwhile, a scattering law was proposed, based on which the developed numerical model could predict the cure widths and cure depths with high accuracy. The developed model can be applied into other photolymerizable ceramic systems such as zirconia, which might trigger more studies for the modeling and simulation of zirconia ceramic.

#### 4.5. Mechanical properties of AM processed zirconia ceramics

Due to the easily induced residual porosity in the obtained components and the flaw-sensitive nature of ceramic materials, most zirconia ceramics processed by AM exhibit inferior mechanical properties compared with those obtained by the traditional methods. It is therefore a major task for the AM processed zirconia ceramics to improve mechanical properties. Numerous efforts have been made to meet this challenge on this front. For instance, Li et al. [171] demonstrated a Ceramic On-Demand Extrusion process for manufacturing dense zirconia ceramic components from aqueous pastes of high solids loading. The as-fabricated 3Y-TZP has a relative density of 98.8%, Vickers hardness of  $13.1 \text{ GPa}$ , fracture toughness of  $4.6 \text{ MPa m}^{1/2}$ , flexural strength of  $616 \text{ MPa}$ , which are much better than those fabricated by other AM processes and close to those from the conventional process. Fu et al. [172] derived the optimum laser power as  $360 \text{ mW}$  for the SLA processing of zirconia ceramic parts, and the corresponding properties are 97% relative density,  $13.1 \text{ GPa}$  hardness,  $5.62 \text{ MPa m}^{1/2}$  fracture toughness and  $1044 \text{ MPa}$  flexural strength. By combining SLA method with gelcasting, the flexural strength and fracture toughness of zirconia-based all-ceramic teeth could reach  $1170 \text{ MPa}$  and  $19.0 \text{ MPa m}^{1/2}$  [107]. The combination of AM techniques with the traditional technique has the potential to manufacture zirconia ceramic with improved mechanical performance. He et al. [96] proposed a novel DLP-stereolithography-based 3D printing process for the fabrication of complex and dense zirconia ceramic parts with Vickers hardness and fracture toughness as  $13.0597 \text{ GPa}$  and  $6.0380 \text{ MPa m}^{1/2}$ , respectively, which are close to the structural properties of zirconia parts fabricated by conventional methods.

#### 4.6. Opportunities

Although AM of zirconia ceramics has tremendous potential, sincere research efforts are further needed to address the aforementioned challenges. The shareholders in the research community and the industry should work closely such that the obstacles can be removed, the niche application areas can

be identified and expanded, and the industry becomes more confident in adopting AM for fabricating zirconia ceramics.

For the existing AM processes capable of making zirconia ceramics, it is believed that the opportunities lie in the following areas. First, the mechanical properties (as well as microstructure) should be improved to close the gap with the traditional methods. In this regard, enhancing the raw material preparation is critical. For instance, in the FDM type of AM process, the stock materials should be prepared with reduced binder material and increased zirconia ceramic powders, and the preparation related techniques must be developed. Also, process optimization is urgently needed to find the best combination of process parameters so that the optimal mechanical properties can be achieved. Second, the studies on the modeling and simulation part of zirconia processing (or for ceramics in general) by AM should be strengthened. Considering that the extensive efforts on modeling and simulation of metal AM [174,175] have greatly helped the maturing of metal AM technology in industry, the similar modeling approaches, such as FEA, phase field modeling, molecular dynamics simulation, and Monte Carlo method, should be adopted. It will not only lead to the better understanding of fundamental mechanisms behind AM of zirconia ceramic, but also help the process and material optimization. Third, the process monitoring and real-time control capability should be developed for AM of zirconia ceramics. It is an area of interest for many AM processes in recent years [176–180]. For ceramic AM, it is even more critical due to the higher level of complexity involved. Fourth, the limitations in the AM equipment should also be overcome such that the zirconia parts of larger sizes, more accurate dimensions, or lower costs can be produced. Lastly, it should be further stressed that the levels of maturity of AM techniques for fabricating zirconia ceramics are different. For the emerging AM techniques, there are generally more challenges and opportunities. For instance, it is recognized that full laser melting of zirconia could produce denser parts compared with SLS, but significant research remains to be conducted to make laser melting a mature process.

Equally important, new AM processes suitable for making zirconia ceramics should be developed. Some of the trials for advanced ceramic AM processing have been reported, such as the combined SLS with sol-gel technique [181], combined DIW with spark plasma sintering [182], freeze-form extrusion [140], and extrusion-based photoreaction method [98,146]. With the fast growth of the application demand, out-of-the-box thinking is strongly encouraged so that new concepts can be cultivated. In this regard, corresponding research on issues such as material preparation, process optimization, and discovery of fundamental mechanisms should be systematically carried out for any newly developed AM processes.

## 5. Conclusion

Zirconia is an important ceramic material, and the fabrication of zirconia components via additive manufacturing has been increasingly investigated by researchers in recent years. The AM techniques used to manufacture zirconia materials focus on selective laser sintering, selective laser melting, stereo-lithography, and ink-jet printing, for which SLA and

IJP have been the mainstream. Other AM techniques, such as binder jetting and 3D gel-printing have also been attempted. This paper offers an extensive review on the current research progress for the additive manufacturing of zirconia ceramic materials and the corresponding applications. More importantly, this paper provides a critical analysis on the challenges and opportunities in the related area.

Regarding the applications of AM produced zirconia parts, aerospace and automotive components, biomedical and fuel cell products, electromagnetic BandGap antenna, electromechanical sensors are the typical examples which have been successfully demonstrated in literature. In certain successful applications, the performance of AM produced zirconia parts exceeds that of traditionally produced parts. However, in terms of mechanical properties such as strengths, AM produced zirconia parts still need to overcome major issues such as cracks and porosities to compete with the traditional manufacturing processes. Each AM method has its own advantages and disadvantages for the zirconia ceramic fabrication. It still remains as a major challenge to figure out a simple, scalable and controllable AM method to produce zirconia parts with high performance. It is believed that the co-existence of various AM methods for fabricating zirconia parts will continue in the foreseeable future.

Although AM of zirconia ceramic materials has witnessed great progress and the potentials are promising, it is not as mature as the AM of metal and polymer materials. Significant challenges remain in terms of raw material development, defect control, and improving mechanical properties of the AM processed zirconia parts. Therefore, the future research should address these challenges and improve the existing AM processes. The hybrid approaches of combining the AM process with other non-AM process deserve more attention. Novel ceramic printing processes and equipment should also be developed. By involving more modeling and simulation techniques into the research of AM of zirconia ceramics, the proper way to achieve zirconia components with high mechanical performance is expected to be derived. It is believed that with sincere efforts, the full potentials of AM produced zirconia can be reached, and more exciting applications can be realized.

## Conflicts of interest

The authors hereby declare that they have no known competing financial interests or personal relationships that could have appeared to influence the work reported in this paper.

## Acknowledgements

The first author would like to recognize that the research work was partially funded by the Xi'an Science and Technology Plan Project (2016CXWL14).

## REFERENCES

- [1] Manicone PF, Iommetti PR, Raffaelli L. An overview of zirconia ceramics: basic properties and clinical applications. *J Dens* 2007;35:819–26.

- [2] Qin W, Majidi H, Yun J, Bentham K. Electrode effects on microstructure formation during flash sintering of yttrium-stabilized zirconia. *J Am Ceram Soc* 2016;99:2253–9.
- [3] Piconi C, Maccauro G. Zirconia as a ceramic biomaterial. *Biomaterials* 1999;20:1–25.
- [4] Kelly JR, Denry I. Stabilized zirconia as a structural ceramic: an overview. *Dent Mater* 2008;24:289–98.
- [5] Chen Y, Moussi J, Drury JL, Wataha JC. Zirconia in biomedical applications. *J Expert Rev Med Dev* 2016;13:945–63.
- [6] Drouin JM, Cales B, Chevalier J, Fantozzi JG. Fatigue behavior of zirconia hip joint heads: experimental results and finite element analysis. *J Biomed Mater Res A* 1997;34:149–55.
- [7] Stefanic M, Krnel K, Pribosic I, Kosmac T. Rapid biomimetic deposition of octacalcium phosphate coatings on zirconia ceramics (Y-TZP) for dental implant applications. *Appl Surf Sci* 2012;258:4649–56.
- [8] Rosentritt M, Kolbeck C, Handel G, Schneider-Feyrer S, Behr M. Influence of the fabrication process on the in vitro performance of fixed dental prostheses with zirconia substructures. *Clin Oral Invest* 2011;15:1007–12.
- [9] Badwal SPS, Ciacchi FT, Zelizko V. The effect of alumina addition on the conductivity, microstructure and mechanical strength of zirconia-yttria electrolytes. *Ionics* 1998;4:25–32.
- [10] Shackelford JF, Doremus RH. Ceramic and glass materials: structure, properties and processing. Springer Science & Business Media; 2008. p. 169–99.
- [11] Thakare V. Progress in synthesis and applications of zirconia. *Int J Eng Rec Dev* 2012;5:25–8.
- [12] Krumov E, Dikova J, Starbova K, Popov D, Blaskov V, Kolev K, et al. Thin  $ZrO_2$  Sol-Gel films for catalytic application. *J Mater Sci-Mater El* 2003;14:759–60.
- [13] Lee JH. Review on zirconia air-fuel ratio sensors for automotive applications. *J Mater Sci* 2003;38:4247–57.
- [14] Sarraf H, Herbig R, Maryska M. Fine-grained  $Al_2O_3-ZrO_2$  composites by optimization of the processing parameters. *Scr Mater* 2008;59:155–8.
- [15] Wang SK, Yu JY, Li Q, Zheng EY, Duan YG, Qi GC. Preparation of gradient ZTA ceramic by centrifugal slip casting method. *Adv Mater Res-Switz* 2012;569:324–7.
- [16] Melendo MJ, Clauss C, Rodriguez AD, Portu GD, Roncari E, Pinasco P. High temperature plastic deformation of multilayered YTZP/ZTA composites obtained by tape casting. *Acta Mater* 1998;46:3995–4004.
- [17] Gadow R, Kern F. Pressureless sintering of injection molded zirconia toughened alumina nanocomposites. *J Ceram Soc Jpn* 2006;114:958–62.
- [18] Beeaff D, Hilmas G. Electrode support structures for planar solid oxide fuel cells. *Key Eng Mater* 2004;264:747–50.
- [19] Rajeswari K, Biswas P, Suresh MB, Hareesh US, Johnson R, Das D. Colloidal shaping of 8 mol% yttria-stabilized zirconia electrolyte honeycomb structures by microwave-assisted thermal gelation of methyl cellulose. *Int J Appl Ceram Technol* 2014;11:154–63.
- [20] Celik S, Timurkutluk B, Toros S, Timurkutluk C. Mechanical and electrochemical behavior of novel electrolytes based on partially stabilized zirconia for solid oxide fuel cells. *Ceram Int* 2015;41:8785–90.
- [21] Ding J, Liu J. A novel design and performance of cone-shaped tubular anode supported segmented-in-series solid oxide fuel cell stack. *J Power Sources* 2009;193:769–73.
- [22] Yu F, Wang H, Bai Y, Yang J. Preparation and characterization of porous  $Si_3N_4$  ceramics prepared by compression molding and slip casting methods. *Bull Mater Sci* 2010;33:619–24.
- [23] Mitteramskogler G, Gmeiner R, Felzmann R, Gruber S, Hofstetter C, Stampfli J, et al. Light curing strategies for lithography-based additive manufacturing of customized ceramics. *Addit Manuf* 2014;1–4:110–8.
- [24] Li WB, Ghazanfari A, McMillen D, Leu MC, Hilmas GE, Watts J. Characterization of zirconia specimens fabricated by ceramic on-demand extrusion. *Ceram Int* 2018;44:12245–52.
- [25] Bhushan B, Caspers M. An overview of additive manufacturing (3D printing) for microfabrication. *Microsyst Technol* 2017;23:1117–24.
- [26] Singha S, Ramakrishnab S, Singhc R. Material issues in additive manufacturing: a review. *J Manuf Process* 2017;25:85–200.
- [27] Deckers J, Vleugels J, Kruth JP. Additive manufacturing of ceramics: a Review. *J Ceram Sci Technol* 2014;5:245–60.
- [28] Lee JM, Sing SL, Zhou M, Yeong WY. 3D bioprinting processes: a perspective on classification and terminology. *Int J Bioprint* 2018;4:151–62.
- [29] Sing SL, Yeong WY, Wiria FE, Tay BY, Zhao Z, Zhao L, et al. Direct selective laser sintering and melting of ceramics: a review. *Rapid Prototyp J* 2017;23:611–23.
- [30] Costa EC, Duarte FP, Bartolo P. A review of additive manufacturing for ceramic production. *Rapid Prototyp J* 2017;23:954–63.
- [31] Galante R, Figueiredo-Pina CG, Serro AP. Additive manufacturing of ceramics for dental applications: A review. *Dent Mater* 2019;35:825–46.
- [32] Hannink RHJ, Kelly PM, Muddle BC. Transformation toughening in zirconia containing ceramics. *J Am Ceram Soc* 2000;83:461–87.
- [33] Cao XQ, Vassen R, Stoever D. Ceramic materials for thermal barrier coatings. *J Eur Ceram Soc* 2004;24:1–10.
- [34] Bonanos N, Slotwinski RK, Steele BCH, Butler EP. High ionic conductivity in polycrystalline tetragonal  $Y_2O_3-ZrO_2$ . *J Mater Soc Lett* 1984;3:245–8.
- [35] Bertrand P, Bayle F, Combe C, Goeuriot P, Smurov I. Ceramic components manufacturing by selective laser sintering. *Appl Surf Sci* 2007;254:989–92.
- [36] Wilkes J, Hagedorn YC, Meiners W, Wissenbach K. Additive manufacturing of  $ZrO_2-Al_2O_3$  ceramic components by selective laser melting. *Rapid Prototyp J* 2013;19:51–7.
- [37] Li J, Craeghs W, Jing C, Gong S, Shan F. Microstructure and physical performance of laser-induction nanocrystalsmodified high-entropy alloy composites on titanium alloy. *Mater Des* 2017;117:363–70.
- [38] Silva JVL, Rezende RA. Additive Manufacturing and its future impact in logistics. *IFAC Proc Vol* 2013;46:277–82.
- [39] Hinczewski C, Corbel S, Chartier T. Ceramic suspensions suitable for stereolithography. *J Eur Ceram Soc* 1998;18:583–90.
- [40] Melchels FPW, Jan F, Grijpma DW. A review on stereolithography and its applications in biomedical engineering. *Biomaterials* 2010;31:6121–30.
- [41] Murphy SV, Atala A. 3D bioprinting of tissues and organs. *Nat Biotechnol* 2014;32:773–85.
- [42] Chang JK, He JK, Mao M, Zhou WX, Lei Q, Li X. Advanced material strategies for next-generation additive manufacturing. *Materials* 2018;11:1–19.
- [43] McEntire BJ, Bala BS, Rahaman MN, Chevalier J, Pezzotti G. Ceramics and ceramic coatings in orthopaedics. *J Eur Ceram Soc* 2015;35:4327–69.
- [44] Nag S, Banerjee R. Fundamentals of medical implant materials. *ASM Handb: Mater Med Dev* 2012;23:6–17.
- [45] Osman RB, Swain MV. A critical review of dental implant materials with an emphasis on titanium versus zirconia. *Materials* 2015;8:932–58.
- [46] Wu H, Liu W, He R, Wu Z, Jiang Q, Song X, et al. Fabrication of dense zirconia-toughened alumina ceramics through a stereolithography-based additive manufacturing. *Ceram Int* 2017;43:968–72.

- [47] Gahlert M, Roehling S, Sprecher CM, Kniha H, Milz S, Bormann K. In vivo performance of zirconia and titanium implants: a histomorphometric study in minipig maxillae. *Clin Oral Implants Res* 2012;23:281–6.
- [48] Ebert J, Özkel E, Zeichner A, Uibel K, Weiss Ö, Koops U, et al. Direct inkjet printing of dental prostheses made of zirconia. *J Dent Res* 2009;88:673–6.
- [49] Christian HY, Jan W, Wilhelm M, Konrad W, Reinhart P. Net shaped high performance oxide ceramic parts by selective laser melting. *Phys Proc* 2010;5:587–94.
- [50] Silva NR, Witek L, Coelho P, Thompson VP, Rekow ED, Smay J. Additive CAD/CAM process for dental prostheses. *J Prosthodont* 2011;20:93–6.
- [51] Lee SY, Jiang CP. Development of a three-dimensional slurry printing system using dynamic mask projection for fabricating zirconia dental implants. *Mater Manuf Process* 2015;30:1498–504.
- [52] Chartier T, Dupas C, Lasgorceix M, Brie J, Champion E, Delhote N, et al. Additive manufacturing to produce complex 3D ceramic parts. *J Ceram Sci Technol* 2015;6:95–104.
- [53] Li Y, Li L, Li B. Direct write printing of three-dimensional  $ZrO_2$  biological scaffolds. *Mater Des* 2015;72:16–20.
- [54] Lian Q, Wu XQ, Li DC, He XN, Meng JL, Liu XD, et al. Accurate printing of a zirconia molar crown bridge using three-part auxiliary supports and ceramic mask projection stereolithography. *Ceram Int* 2019;45:18814–22.
- [55] Osman RB, Veen AJ, Huiberts D, Wismeijer D, Alharbi N. 3D-printing zirconia implants; a dream or a reality? An in-vitro study evaluating the dimensional accuracy, surface topography and mechanical properties of printed zirconia implant and discs. *J Mech Behav Biomed Mater* 2017;75:521–8.
- [56] Soshu K. Creation of functional ceramic structures by using stereolithographic 3D printing. *Trans JWRI* 2014;43:5–10.
- [57] Delhote N, Bila S, Baillargeat D, Chartier T, Verdeyme S. Advanced design and fabrication of microwave components based on shape optimization and 3D ceramic stereolithography process. In: Advances in ceramic – synthesis and characterization, processing and specific applications. 2011. p. 243–76.
- [58] Yan S, Wu DJ, Niu FY, Ma GY, Kang RK.  $Al_2O_3$ - $ZrO_2$  eutectic ceramic via ultrasonic-assisted laser engineered net shaping. *Ceram Int* 2017;43:15905–10.
- [59] Farando NM, Li T, Kelsall GH. 3-D inkjet-printed solid oxide electrochemical reactors. II. LSM - YSZ electrodes. *Electrochim Acta* 2018;270:264–73.
- [60] Xu Y, Wu X, Guo X, Kong B, Zhang M, Qian X, et al. The boom in 3D-printed sensor technology. *Sensors* 2017;7:1166–203.
- [61] Han T, Kundu S, Nag A, Xu Y. 3D printed sensors for biomedical applications: a review. *Sensors* 2019;19:1706.
- [62] Jafari M, Han W, Mohammadi F, Safari A, Danforth S, Langrana N. A novel system for fused deposition of advanced multiple ceramics. *Rapid Prototyp J* 2000;6:161–75.
- [63] Beaman JJ, Deckard CR. Selective laser sintering with assisted powder handling. United States Patent 4, 938, 816. 1990 [patent].
- [64] Shahzad K, Deckers J, Kruth JP, Vleugels J. Additive manufacturing of alumina parts by indirect selective laser sintering and post processing. *J Mater Process Technol* 2013;213:1484–94.
- [65] Deckers J, Meyers S, Kruth JP, Vleugels J. Direct selective laser sintering melting of high density alumina powder layers at elevated temperatures. *Phys Proc* 2014;56: 117–24.
- [66] Travitzky N, Bonet A, Dermeik B, Fey T, Demut IF, Schlier L. Additive manufacturing of ceramic-based materials. *Adv Eng Mater* 2014;16:729–54.
- [67] Danezan A, Delaizir G, Tessier-Doyen N, Gasgnier G, Gaillard JM, Duport P. Selective laser sintering of porcelain. *J Eur Ceram Soc* 2018;38:769–75.
- [68] Gureev DM, Ruzhechko RV, Shishkovski IV. Selective laser sintering of PZT ceramic powders. *Tech Phys Lett* 2000;26:262–4.
- [69] Klocke F, Derichs C, Ader C, Demmer A. Investigations on laser sintering of ceramic slurries. *Prod Eng* 2007;279–84.
- [70] Mühlér T, Heinrich J. Slurry-based additive manufacturing of ceramics. *Int J Appl Ceram Technol* 2015;12:18–25.
- [71] Wu Y, Du J, Choy KL, Hench LL. Laser densification of powder beds generated using aerosol assisted spray deposition. *J Eur Ceram Soc* 2007;27:4727–35.
- [72] Shahzad K, Deckers J, Zhang Z, Kruth JP, Vleugels J. Additive manufacturing of zirconia parts by indirect selective laser sintering. *J Eur Ceram Soc* 2014;34:81–9.
- [73] Cardon L, Deckers J, Verberckmoes A, Ragaert K, Delva L, Shahzad K, et al. Polystyrene-coated alumina powder via dispersion polymerization for indirect selective laser sintering applications. *J Appl Polym Sci* 2013;128:2121–8.
- [74] Deckers J, Kruth JP, Shahzad K, Vleugels J. Density improvement of alumina parts produced through selective laser sintering of alumina-polyamide composite powder. *CIRP Ann Manuf Technol* 2012;61:211–4.
- [75] Ferrage L, Bertrand G, Lenormand P. Dense yttria-stabilized zirconia obtained by direct selective laser sintering. *Addit Manuf* 2018;21:472–8.
- [76] Shirazi SFS, Gharehkhani S, Mehrali M, Yarmand H, Metselaar HSC, Kadri NA, et al. A review on powder-based additive manufacturing for tissue engineering: selective laser sintering and inkjet 3D printing. *Sci Technol Adv Mater* 2015;16:1–17.
- [77] Slocombe A, Li L. Selective laser sintering of  $TiC$ - $Al_2O_3$  composite with self-propagating high-temperature synthesis. *J Mater Process Technol* 2001;118:173–8.
- [78] Chen Z, Li Z, Li J, Liu C, Lao C, Fu Y, et al. 3D printing of ceramics: a review. *J Eur Ceram Soc* 2019;39:661–87.
- [79] Shishkovsky I, Yadroitsev I, Bertrand P, Smurov I. Alumina-zirconium ceramics synthesis by selective laser sintering/melting. *Appl Surf Sci* 2007;254:966–70.
- [80] Niu F, Wu D, Ma G, Wang J, Guo M, Zhang B. Nanosized microstructure of  $Al_2O_3$ - $ZrO_2$ ( $Y_2O_3$ ) eutectics fabricated by laser engineered net shaping. *Scr Mater* 2015;95: 39–41.
- [81] Liu Q, Danlos Y, Song B, Zhang BC, Yin S, Liao HL. Effect of high-temperature preheating on the selective laser melting of yttria-stabilized zirconia ceramic. *J Mater Process Technol* 2015;222:61–74.
- [82] Liu Z, Song K, Gao B, Tian T, Yang H, Lin X, et al. Microstructure and mechanical properties of  $Al_2O_3$ / $ZrO_2$  directionally solidified eutectic ceramic prepared by laser 3D printing. *J Mater Soc Technol* 2016;32:320–5.
- [83] Liu H, Su H, Shen Z, Wang E, Zhao D, Guo M, et al. Direct formation of  $Al_2O_3$ / $GdAlO_3$ / $ZrO_2$  ternary eutectic ceramics by selective laser melting: microstructure evolutions. *J Eur Ceram Soc* 2018;38:5144–52.
- [84] Yang MM, Luo XD, Xie ZP. Review of 3D printing technology of ceramic. *J Synth Cryst (China)* 2017;46:183–6.
- [85] Lian Q, Sui WQ, Wu XQ, Yang F, Yang SP. Additive manufacturing of  $ZrO_2$  ceramic dental bridges by stereolithography. *Rapid Prototyp J* 2018;24:114–9.
- [86] Masciandaro S, Torrell M, Tarancón LPA. Three-dimensional printed yttria-stabilized zirconia self-supported electrolytes for solid oxide fuel cell applications. *J Eur Ceram Soc* 2019;39:9–16.
- [87] Rosa M, Barou C, Esposito V. Zirconia UV-curable colloids for additive manufacturing via hybrid inkjet printing-stereolithography. *Mater Lett* 2018;215:214–7.

- [88] Song SY, Park MS, Lee D, Lee JW, Yun JS. Optimization and characterization of high-viscosity ZrO<sub>2</sub> ceramic nanocomposite resins for supportless stereolithography. *Mater Des* 2019;180:107960.
- [89] Liu K, Zhang K, Bourell DL, Chen F, Sun H, Shi Y, et al. Gelcasting of zirconia-based all-ceramic teeth combined with stereolithography. *Ceram Int* 2018;44:21556–63.
- [90] Griffith ML, Halloran JW. Freeform fabrication of ceramics via stereolithography. *J Am Ceram Soc* 1996;79:2601–8.
- [91] Sun JX, Binner J, Bai JM. Effect of surface treatment on the dispersion of nano zirconia particles in non-aqueous suspensions for stereolithography. *J Eur Ceram Soc* 2019;39:1660–7.
- [92] Song X, Chen Y, Lee TW, Wu SH, Cheng LX. Ceramic fabrication using mask-image-projection-based stereolithography integrated with tape-casting. *J Manuf Process* 2015;20:456–64.
- [93] Wu ZW, Liu W, Wu HD, Huang RJ, He RX, Jiang QG, et al. Research into the mechanical properties, sintering mechanism and microstructure evolution of Al<sub>2</sub>O<sub>3</sub>-ZrO<sub>2</sub> composites fabricated by a stereolithography-based 3D printing method. *Mater Chem Phys* 2018;207:1–10.
- [94] Bae CJ, Halloran JW. Concentrated suspension-based additive manufacturing-viscosity, packing density, and segregation. *J Eur Ceram Soc* 2019;34:1016.
- [95] Zhang L, Chen SF, Shen Y, Lu DF, Guo QS. Optimization research on forming of fine alumina ceramic by hydrous gel-casting. *Inform Midem* 2005;24:44–7.
- [96] He RX, Liu W, Wu ZW, An D, Huang MP, Wu HD, et al. Fabrication of complex-shaped zirconia ceramic parts via a DLP-stereolithography-based 3D printing method. *Ceram Int* 2018;44:3412–6.
- [97] Jiang CP, Hsu HJ, Lee SY. Development of mask-less projection slurry stereolithography for the fabrication of zirconia dental coping. *Int J Precis Eng Manuf* 2014;15:2413–9.
- [98] Zhang K, He R, Xie C, Wang G, Ding G, Wang M, et al. Photosensitive ZrO<sub>2</sub> suspensions for stereolithography. *Ceram Int* 2019;45:12189–95.
- [99] Halloran JW. Ceramic stereolithography: additive manufacturing for ceramics by photopolymerization. *Ann Rev Mater Res* 2016;46:19–40.
- [100] Faes M, Valkenaers H, Vogeler F, Vleugels J, Ferraris E. Extrusion-based 3D printing of ceramic components. *Proc CIRP* 2015;28:76–81.
- [101] Li XB, He Z, Zhang JX, Duan YS, Bai HN, Li JJ, et al. Dispersion and properties of zirconia suspensions for stereolithography. *Int J Appl Ceram Technol* 2020;17: 239–47.
- [102] Wu HD, Liu W, Huang RJ, He RX, Huang MP, An D, et al. Fabrication of high-performance Al<sub>2</sub>O<sub>3</sub>-ZrO<sub>2</sub> composite by a novel approach that integrates stereolithography-based 3D printing and liquid precursor infiltration. *Mater Chem Phys* 2018;209:31–7.
- [103] Badev A, Aboualiatim Y, Chartier T, Lecamp L, Lebaudy P, Chaput C, et al. Photopolymerization kinetics of a polyether acrylate in the presence of ceramic fillers used in stereolithography. *J Photochem Photobiol A* 2011;222:117–22.
- [104] Wozniak M, Graule T, Hazan Y, Kata D, Lis J. Highly loaded UV curable nanosilica dispersions for rapid prototyping applications. *J Eur Ceram Soc* 2009;29:2259–65.
- [105] Corcione CE, Greco A, Maffezzoli A. Temperature evolution during stereolithography building with a commercial epoxy resin. *Polym Eng Sci* 2006;46:493–502.
- [106] Wang JC, Dommati H. Fabrication of zirconia ceramic parts by using solvent-based slurry stereolithography and sintering. *Int J Adv Manuf Technol* 2018;98:1537–46.
- [107] Xing HY, Zou B, Li SS, Fu XS. Study on surface quality, precision and mechanical properties of 3D printed ZrO<sub>2</sub> ceramic components by laser scanning stereolithography. *Ceram Int* 2017;3:16340–7.
- [108] Liu X, Zou B, Xing H, Huang C. The preparation of ZrO<sub>2</sub>-Al<sub>2</sub>O<sub>3</sub> composite ceramic by SLA-3D printing and sintering processing. *Ceram Int* 2020;46:937–44.
- [109] Bae CJ, Halloran JW. Influence of residual monomer on cracking in ceramics fabricated by stereolithography. *Int J Appl Ceram Technol* 2011;8:1289–95.
- [110] Schmidt J, Colombo P. Digital light processing of ceramic components from polysiloxanes. *J Eur Ceram Soc* 2018;38:57–66.
- [111] Schwentwein M, Homa J. Additive manufacturing of dense alumina ceramics. *Int J Appl Ceram Technol* 2015;12:1–7.
- [112] Hatzenbichler M, Geppert M, Gruber S, Ipp E, Almedal R, Stampfli J. DLP-based light engines for additive manufacturing of ceramic parts. In: Emerging digital micromirror device based systems and applications IV. San Francisco, California, United States: International Society for Optics and Photonics; 2012. p. 8254.
- [113] Komissarenko DA, Sokolov PS, Evstigneeva AD, Shmeleva IA, Dosovitsky AE. Rheological and curing behavior of a crylate-based suspensions for the DLP 3D printing of complex zirconia parts. *Materials* 2018;11:2350–62.
- [114] Zhang KQ, He RJ, Ding GJ, Feng CW, Xia M, Song WD, et al. Digital light processing of 3Y-TZP strengthened ZrO<sub>2</sub> ceramics. *Mater Sci Eng A* 2020;774:138768.
- [115] Lewis JA, Smay JE, Stuecker J, Cesario J. Direct ink writing of three-dimensional ceramic structures. *J Am Ceram Soc* 2006;89:3599–609.
- [116] Derby B. Additive manufacture of ceramics components by inkjet printing. *Engineering* 2015;1:113–23.
- [117] Blazdell P, Evans J, Edirisinghe M, Shaw P, Binstead M. The computer aided manufacture of ceramics using multilayer jet printing. *J Mater Sci Lett* 1995;14:1562–5.
- [118] Tomov RI, Krauz M, Jewulski J, Hopkins SC, Kluczowski JR, Glowacka DM, et al. Direct ceramic inkjet printing of yttria-stabilized zirconia electrolyte layers for anode-supported solid oxide fuel cells. *J Power Sources* 2010;195:7160–7.
- [119] Özkol E, Wätjen AM, Bermejo R, Deluca M, Ebert J, Danzer R, et al. Mechanical characterisation of miniaturised direct inkjet printed 3Y-TZP specimens for microelectronic applications. *J Eur Ceram Soc* 2010;30:3145–52.
- [120] Esposito V, Gadea C, Hjelm J, Marani D, Hu Q, Agersted K, et al. Fabrication of thin yttria-stabilized-zirconia dense electrolyte layers by inkjet printing for high performing solid oxide fuel cells. *J Power Sources* 2015;273:89–95.
- [121] Farandos NM, Kleiminger L, Li, Hankin A, Kelsall GH. Three-dimensional Inkjet Printed Solid Oxide Electrochemical Reactors. I. Yttria-stabilized Zirconia Electrolyte. *Electrochim Acta* 2016;213:324–31.
- [122] Özkol E, Ebert J, Telle R. An experimental analysis of the influence of the ink properties on the drop formation for direct thermal inkjet printing of high solid content aqueous 3Y-TZP suspensions. *J Eur Ceram Soc* 2010;30:1669–78.
- [123] Özkol E. Rheological characterization of aqueous 3Y-TZP inks optimized for direct thermal ink-jet printing of ceramic components. *J Am Ceram Soc* 2013;9:1124–30.
- [124] Özkol E, Zhang W, Ebert J. Potentials of the “inkjet printing” direct method for manufacturing 3Y-TZP based dental restoration. *J Eur Ceram Soc* 2012;32:2193–201.
- [125] Derby B. Inkjet printing ceramics: from drops to solid. *J Eur Ceram Soc* 2011;31:2543–50.
- [126] Derby B, Reis N. Inkjet printing of highly loaded particulate suspensions. *MRS Bull* 2003;28:815–8.

- [127] Özkol E, Ebert J, Uibel K, Wätjen AM, Telle R. Development of high solid content aqueous 3Y-TZP suspensions for direct inkjet printing using a thermal inkjet printer. *J Eur Ceram Soc* 2009;29:403–9.
- [128] Smith P, Derby B, Reis N, Wallwork A, Ainsley C. Measured anisotropy of alumina components produced by direct ink-jet printing. *Key Eng Mater* 2005;264:693–6.
- [129] Noguera R, Lejeune M, Chartier T. 3D fine scale ceramic components formed by ink-jet prototyping process. *J Eur Ceram Soc* 2005;25:2055–9.
- [130] Gingter P, Watjen AM, Kramer M. Functionally graded ceramic structures by direct thermal inkjet printing. *J Ceram Sci Technol* 2015;6:119–24.
- [131] Wang TM, Derby B. Ink-jet printing and sintering of PZT. *J Am Ceram Soc* 2005;88:2053–8.
- [132] Rosa M, Gooden PN, Butterworth S, Zielke P, Kiebach R, Xu Y, et al. Zirconia nano-colloids transfer from continuous hydrothermal synthesis to inkjet printing. *J Eur Ceram Soc* 2019;39:2–8.
- [133] Deegan RD, Bakajin O, Dupont TF, Huber G, Nagel SR, Witten TA. Capillary flow as the cause of ring stains from dried liquid drops. *Nature* 1997;389:827–9.
- [134] Majumder M, Rendall CS, Eukel JA, Wang JY, Behabtu N, Pint CL, et al. Overcoming the “coffee-stain” effect by compositional Marangoni-flow-assisted drop-drying. *J Phys Chem B* 2012;116:6536–42.
- [135] Dou R, Wang T, Guo Y, Derby B. Ink-jet printing of zirconia: coffee staining and line stability. *J Am Ceram Soc* 2011;94:3787–92.
- [136] Friederich A, Binder JR, Bauer W. Rheological control of the coffee stain effect for inkjet printing of ceramics. *J Am Ceram Soc* 2013;96:2093–9.
- [137] Dou R, Derby B. Formation of coffee stains on porous surfaces. *Langmuir* 2012;28:5331–8.
- [138] Zhao HP, Ye CS, Fan ZT, Shi YN. 3D printing of  $ZrO_2$  ceramic using nano-zirconia suspension as a binder. *Proc 2015 4th Int Conf Sensors, Meas Intell Mater* 43 2016:654–7.
- [139] Shao H, Zhao D, Lin T, He J, Wu J. 3D gel-printing of zirconia ceramic parts. *Ceram Int* 2017;43:13938–42.
- [140] Leu MC, Deuser BK, Tang L, Landers RG, Hilmas GE, Watts JL. Freeze-form extrusion fabrication of functionally graded materials. *CIRP Ann* 2012;61:223–6.
- [141] Scheithauer U, Johne R, Weingarten S, Schwarzer E, Richter HJ, Moritz T, et al. Investigation of droplet deposition for suspensions usable for thermoplastic 3D printing (T3DP). *J Mater Eng Perform* 2018;27:44–51.
- [142] Scheithauer U, Weingarten S, Johne R, Schwarzer E, Abel J, Richter HJ, et al. Ceramic-based 4D components: additive manufacturing (AM) of ceramic-based functionally graded materials (FGM) by thermoplastic 3D printing (T3DP). *Materials* 2017;10:1368–87.
- [143] Ghazanfari A, Li W, Leu MC, Watts JL, Hilmas GE. Additive manufacturing and mechanical characterization of high density fully stabilized zirconia. *Ceram Int* 2017;43:6082–8.
- [144] Peng E, Wei X, Garbe U, Yu D, Edouard B, Liu A, et al. Robocasting of dense yttria-stabilized zirconia structures. *J Mater Sci* 2018;53:247–73.
- [145] Liao J, Chen H, Luo H, Wang X, Zhou K, Zhang D. Direct ink writing of zirconia three-dimensional structures. *J Mater Chem C* 2017;5:5867–71.
- [146] Faes M, Vleugels J, Vogeler F, Ferraris E. Extrusion-based additive manufacturing of  $ZrO_2$  using photoinitiated polymerization. *CIRP Manuf Sci Technol* 2016;14:28–34.
- [147] Yu T, Zhang Z, Liu Q, Kuliev R, Orlovskaya N, Wu D. Extrusion-based additive manufacturing of yttria-partially-stabilized zirconia ceramics. *Ceram Int* 2020;46:5020–7.
- [148] Zocca A, Colombo P, Gomes CM, Gunster J. Additive manufacturing of ceramics: issues, potentialities, and opportunities. *J Am Ceram Soc* 2015;98:1983–2001.
- [149] Lewis JA. Direct-write assembly of ceramics from colloidal inks. *Curr Opin Solid St Mech* 2002;6:245–50.
- [150] Manogharan G, Kioko M, Linkous C. Binder jetting: a novel solid oxide fuel-cell fabrication process and evaluation. *JOM* 2015;67:660–7.
- [151] Ceserano I, Segalman R. Robocasting provides moldless fabrication from slurry deposition. *Ceram Ind* 1998;148:94–100.
- [152] Fu Q, Saiz E, Tomsia AP. Direct ink writing of highly porous and strong glass scaffolds for load-bearing bone defects repair and regeneration. *Acta Biomater* 2011;7:3547–54.
- [153] Yu TY, Zhang ZY, Liu QY, Kuliev R, Orlovskaya N, Wu D. Extrusion-based additive manufacturing of yttria-partially-stabilized zirconia ceramics. *Ceram Int* 2020;46:5020–7.
- [154] Yang L, Miyanaji H. Ceramic additive manufacturing: a review of current status and challenges. *Proceedings of the 28th annual international solid freeform fabrication symposium – an additive manufacturing conference* 2017:652–79.
- [155] Sing SL, An J, Yeong WY, Wiria FE. Laser and electron-beam powder-bed additive manufacturing of metallic implants: a review on processes, materials and designs. *J Orthop Res* 2016;34:369–85.
- [156] Bourell D, Kruth JP, Leu M, Levy G, Rosen D, Beese AM, et al. Materials for additive manufacturing. *CIRP Ann Manuf Technol* 2017;66:659–81.
- [157] Bienia M, Lejeune M, Chambon M, Baco-Carles V, Dossou-Yovo C, Noguera R, et al. Inkjet printing of ceramic colloidal suspensions: filament growth and breakup. *Chem Eng Sci* 2016;149:1–13.
- [158] Vorndran E, Klärner M, Klammert U, Grover LM, Patel S, Barralet JE, et al. 3D powder printing of  $\beta$ -tricalcium phosphate ceramics using different strategies. *Adv Eng Mater* 2018;10:67–71.
- [159] Sun C, Tian X, Wang L, Liu Y, Wirth CM, Günster J, et al. Effect of particle size gradation on the performance of glass-ceramic 3D printing process. *Ceram Int* 2017;43:578–84.
- [160] Dehurtevent M, Robberecht L, Hornez JC, Thuault A, Deveaux E, Béhin P. Stereolithography: a new method for processing dental ceramics by additive computer-aided manufacturing. *Dent Mater* 2017;33:77–485.
- [161] Wong KV, Hernandez A. A review of additive manufacturing. *ISRN Mech Eng* 2012;1:1–10.
- [162] Gokhare VG, Raut DN, Shinde DK. A review paper on 3D-printing aspects and various processes used in the 3D-printing. *Int J Eng Res Technol* 2017;6:953–8.
- [163] Ngo TD, Kashani A, Imbalzano G, Nguyen KTQ, Hui D. Additive manufacturing (3D printing): a review of materials, methods, applications and challenges. *Compos Pt B-Eng* 2018;143:172–96.
- [164] Su B, Dhara S, Wang L. Green ceramic machining: a top-down approach for the rapid fabrication of complex-shaped ceramics. *J Eur Ceram Soc* 2008;28:2109–15.
- [165] Bae CJ, Halloran JW. Integrally cored ceramic mold fabricated by ceramic stereolithography. *Int J Appl Ceram Technol* 2011;8:1255–62.
- [166] Deckers J, Kruth JP, Cardon L, Shahzad K, Vleugels J. Densification and geometrical assessments of alumina parts produced through indirect selective laser sintering of alumina-polystyrene composite powder. *Stroj Venstn J Mech* 2013;59:646–61.
- [167] Pham TA, Kim DP, Lim TW, Park SH, Yang DY, Lee KS. Three-dimensional SiCN ceramic microstructures via

- nano-stereolithography of inorganic polymer photoresists. *Adv Funct Mater* 2006;16:1235–41.
- [168] Abouliatim Y, Chartier T, Abelard P, Chaput C, Delage G. Optical characterization of stereolithography alumina suspensions using the Kubelka–Munk model. *J Eur Ceram Soc* 2009;29:919–24.
- [169] Chen SB, Li DC, Tian XY, Wang MJ, Dai W. Effective fabrication method of 3D ceramic photonic crystals with diamond structure. *Rapid Prototyp J* 2012;18:49–55.
- [170] Tarabeux J, Pateloup V, Michaud P, Chartier T. Development of a numerical simulation model for predicting the curing of ceramic systems in the stereolithography process. *J Eur Ceram Soc* 2018;38:4089–98.
- [171] Li WB, Ghazanfari A, McMillen D, Leu MC, Hilmas GE, Watts J. Properties of partially stabilized zirconia components fabricated by the ceramic on-demand extrusion process. *Proceedings of the 27th annual international solid freeform fabrication symposium* 2016:916–28.
- [172] Fu X, Zou B, Xing H, Li L, Li Y, Wang X. Effect of printing strategies on forming accuracy and mechanical properties of ZrO<sub>2</sub> parts fabricated by SLA technology. *Ceram Int* 2019;45:17630–7.
- [174] Stavropoulos P, Foteinopoulos P. Modelling of additive manufacturing processes: a review and classification. *Manuf Rev* 2018;5:1–26.
- [175] Khanafar K, Masri AA, Aithal S, Deiab I. Multiphysics modeling and simulation of laser additive manufacturing process. *Int J Des Manuf* 2019;13:537–44.
- [176] Spears TG, Gold SA. In-process sensing in selective laser melting (SLM) additive manufacturing. *Integr Mater Manuf Innov* 2016;5:16–40.
- [177] Chua ZY, Ahn H, Moon SK. Process monitoring and inspection systems in metal additive manufacturing: Status and applications. *Int J Precis Eng Manuf-Green Technol* 2017;4:235–45.
- [178] Lu QY, Wong CH. Additive manufacturing process monitoring and control by non-destructive testing techniques: challenges and in-process monitoring. *Virtual Phys Prototyp* 2018;13:39–48.
- [179] Mani M, Lane BM, Donmez MA, Feng SC, Moylan SP. A review on measurement science needs for real-time control of additive manufacturing metal powder bed fusion processes. *Int J Prod Res* 2017;55:1400–18.
- [180] Tapia G, Eiwany A. A review on process monitoring and control in metal-based additive manufacturing. *J Manuf Sci Eng* 2014;136:060801.
- [181] Liu FH, Shen YK, Liao YS. Selective laser gelation of ceramic-matrix composites. *Compos B Eng* 2011;42:57–61.
- [182] Eqtesadi S, Motealleh A, Perera FH, Miranda P, Pajares A, Wendelbo R, et al. Fabricating geometrically-complex B<sub>4</sub>C ceramic components by robocasting and pressureless spark plasma sintering. *Scr Mater* 2018;145:14–8.